KINETIC STUDIES OF THERMAL AND CATALYTIC CRACKING OF LIGHT HYDROCARBONS

KIYOSHI KUBOTA and NORIYOSHI MORITA

Department of Chemical Engineering

(Received May 31, 1971)

CONTENTS

Nomenclature

C_j : concentration of j-th component [mol/cc]
d : inside diameter, d' : outside diameter [cm] or [m]
F : molar flow rate [mol/sec] or [kg-mol/hr]
k : rate constant (rate parameter) [consistent unit]
l : length of one section or one tube [cm] or [m]
N_j : moles of j-th component based on 100 moles of feed reactant [mol] or [kg-mol]
n : order of reaction [−]
P : total pressure [atm]
q : heat flux supplied to wall [kcal/hr·m^2]
R : gas constant [cc·atm/mol·deg] or [m^3·atm/kg-mol·deg]
r : rate of elementary reaction [mol/sec·cc]
$\Re_j$: rate of reaction of j-th component [mol/sec·cc] or [mol/sec·g-cat]
s : dimensionless length of reactor based on l [−]
T : temperatur [°K]
$V=N_tRT/P$: total volume of gases based on 100 moles of feed reactant gas [cc] or [m^3]
W : mass of catalyst [g-cat]
X_A : conversion of key compornent [−]
y_j : mol fraction of j-th component in reacting gases [−]
$\hat{y}_j$: molar percentage of j-th compornent measured by gas chromatography [mol%]
ε_A : expansion factor of reaction [−]
θ : time [sec], τ : time [hr]
σ_{N_j} : standard deviation of N_j [mol]

Subscripts

i : number of experimental point (I=total number)

j : number of compornent (J=total number)
j=A: key compornent (propane or butane), i-A: iso-butane, B: butane, D: butenes, F: propane, P: propylene, E: ethane, Q: ethylene, M: methane, H: hydrogen, C: coke, S: steam
n : number of tube (n_E=total number)
o : initial value, t : total value
obs : observed value, calc : calculated value
p, q : number of parameter (P=total number)

Introduction

Thermal cracking of light hydrocarbons such as methane, ethane, propane, and butane has been studied by many authors mainly in connections with the overall rate of reactant conversion, mean composition of products, and the free radical mechanisms of elementary reactions. Thus, researches of the free radical mechanisms were presented by Snow *et al.*[42] and Laidler *et al.*[23] on ethane pyrolysis, by Kunugi *et al.*[21)22)] on ethylene, by Laidler *et al.*[23)24)], Tominaga *et al.*[44)], and Amano *et al.*[1)] on propane and propylene, and by Purnell *et al.*[35)] and Wang *et al.*[46)] on butane. In contrast, quantitative investigation of the rates of formation of cracking products and their changes with progress in reaction are rather rare.

For detailed design of cracking furnaces, stoichiometric relations between reactants and products and quantitative expressions for the rates of production of essential products are required. With these relations, we can make decisions of furnace size, feed rate, heat supply, maximum allowable temperature, and so on, to optimize the cracking process. For the thermal cracking of propane, Lichtenstein[25)] introduced the stoichiometric equations and the rate equations as shown in Table 1. Following four primary reactions, he introduced four secondary reactions and one tertiary reaction with complicated stoichiometric coefficients obtained experimentally. Hirado *et al.*[11)] calculated product distributions using

TABLE 1. Stoichiometric Equations of Propane Pyrolysis Presented by Lichtenstein[25)]

primary reactions
$C_3H_8 \rightarrow C_2H_4 + CH_4$
$2\,C_3H_8 \rightarrow C_2H_6 + C_3H_6 + CH_4$
$C_3H_8 \rightleftarrows C_3H_6 + H_2$
$2\,C_3H_8 \rightleftarrows C_2H_6 + C_4H_{10}$
secondary reaction
$C_3H_6 \rightarrow 0.149\,CH_4 + 0.064\,C_2H_2 + 0.2555\,C_2H_4 + 0.085\,C_5H_{10} + 0.2555\,C_4H_8 + 0.0745\,C_6H_{12} + 0.0745\,H_2 + 0.053\,C_2H_6 + 0.053\,C_4H_6$
$C_4H_{10} \rightarrow 0.12\,H_2 + 0.49\,CH_4 + 0.39\,C_2H_4 + 0.38\,C_2H_6 + 0.49\,C_3H_6 + 0.01\,C_3H_8 + 0.12\,C_4H_8$
$C_2H_6 \rightleftarrows C_2H_4 + H_2$
$C_4H_8 + H_2 \rightarrow CH_4 + C_3H_6$
tertiary reaction
$0.287\,C_2H_2 + 0.333\,C_6H_{12} + 0.38\,C_5H_8 \rightarrow 0.472\,C_6H_6 + 0.91\,CH_4 + 0.333\,C_2H_4 + 0.178\,C$

the four stoichiometric equations as shown in Table 2, assuming first-order of each reaction. These equations were so simple as they represented experimental results poorly.

TABLE 2. Stoichiometric Equations of Propane Pyrolysis Presented by Hirado *et al.*[11]

$C_3H_8 \rightarrow C_2H_4 + CH_4$
$C_3H_8 \rightarrow C_3H_6 + H_2$
$C_3H_8 \rightarrow C_2H_6 + 0.5\ C_2H_4$
$C_3H_6 \rightarrow 0.5\ C_mH_n + CH_4$

In the present report, a set of stoichiometric equations and a set of rate equations, which can be conveniently applied for furnace design, are developed in Chapter 1 for pyrolysis of propane, based on free radical mechanisms adopted from many authors. In Chapter 2, experimental results of pyrolysis of propane are presented and discussed. Methods to estimate optimum values of parameters in the rate equations are investigated in Chapter 3 and evaluated by the use of the experimental results. A method to design a tubular pyrolysis unit is presented in Chapter 4 to show the applicability of the rate equations. The same methods are applied to the catalytic cracking of butane in Chapter 5.

1. Derivation of Stoichiometric Equations and Rate Equations of Propane Pyrolysis[14]

1.1 Elementary free radical reactions of propane pyrolysis

The free radical mechanism of propane pyrolysis is postulated as in Table 3,

TABLE 3. Elementary Free Radical Reactions and Rate Equations for Propane Pyrolysis

Elementary free radical reaction	Rate equation	
low conversion level:		
initiation step		
$C_3H_8 \rightarrow C_2H_5\cdot + CH_3\cdot$	$r_1 = k_1 C_A$	(1)
propagation step		
$C_2H_5\cdot + C_3H_8 \rightarrow C_2H_6 + C_3H_7\cdot$	$r_2 = k_2 C_A C_{E\cdot}$	(2)
$C_2H_5\cdot \rightarrow C_2H_4 + H\cdot$	$r_3 = k_3 C_{E\cdot}$	(3)
$CH_3\cdot + C_3H_8 \rightarrow CH_4 + C_3H_7\cdot$	$r_4 = k_4 C_A C_{M\cdot}$	(4)
$C_3H_7\cdot \rightarrow C_2H_4 + CH_3\cdot$	$r_5 = k_5 C_{A\cdot}$	(5)
$H\cdot + C_3H_8 \rightarrow H_2 + C_3H_7\cdot$	$r_6 = k_6 C_A C_{H\cdot}$	(6)
$C_3H_7\cdot \rightarrow C_3H_6 + H\cdot$	$r_7 = k_7 C_{A\cdot}$	(7)
termination step		
$C_3H_7\cdot + CH_3\cdot \rightarrow C_3H_6 + CH_4$	$r_8 = k_8 C_{A\cdot} C_{M\cdot}$	(8)
$2\ CH_3\cdot \rightarrow C_2H_6$	$r_9 = k_9 C_{M\cdot}^2$	(9)
high conversion level:		
propagation step		
$H\cdot + C_2H_4 \rightleftarrows C_2H_5\cdot{}^*$	$r_{10} = k_{10} C_Q C_{H\cdot}$	(10)
$H\cdot + C_3H_6 \rightleftarrows C_3H_7\cdot{}^* \rightarrow C_2H_4 + CH_3\cdot$	$r_{11} = k_{11} C_P C_{H\cdot}$	(11)
$CH_3\cdot + C_2H_4 \rightleftarrows C_3H_7\cdot{}^* \rightarrow C_3H_6 + H\cdot$	$r_{12} = k_{12} C_Q C_{M\cdot}$	(12)
$CH_3\cdot + C_3H_6 \rightleftarrows C_4H_9\cdot{}^* \rightarrow C_2H_4 + C_2H_5\cdot$	$r_{13} = k_{13} C_P C_{M\cdot}$	(13)
$H\cdot + C_3H_6 \rightarrow H_2 + C_3H_5\cdot$	$r_{14} = k_{14} C_P C_{H\cdot}$	(14)
$CH_3\cdot + C_3H_6 \rightarrow CH_4 + C_3H_5\cdot$	$r_{15} = k_{15} C_P C_{M\cdot}$	(15)
$C_3H_5\cdot + C_3H_6 \rightleftarrows C_6H_{11}\cdot{}^* \rightarrow$ polymer $+ H\cdot$	$r_{16} = k_{16} C_P C_{P\cdot}$	(16)
termination step		
$C_3H_5\cdot + CH_3\cdot \rightarrow C_4H_8$	$r_{17} = k_{17} C_{P\cdot} C_{M\cdot}$	(17)

referring to the mechanisms proposed by Laidler *et al.*[24] and Tominaga *et al.*[44] Here, the secondary reactions at high conversion level are selected according to the following reasonings. The methyl radicals and hydrogen atom are formed mainly by the propagation reactions (4)~(7) and are important reactive intermediates at high conversion level. They cause addition reactions with ethylene and propylene, and cause hydrogen atom abstraction reaction with propylene, which has lower hydrogen-carbon bond energy than propane. Free radicals other than allyl cause hydrogen atom abstraction reactions with propane and restore to molecules, while allyl radical is stable at the presence of propane and formes allene or polymers. As the allene was not observed in our experiments, we assumed the production of polymers. We also assume the termination reaction of allyl radical with methyl radical.

TABLE 4. Rate Equations of Production of Stable Molecular Species

$\Re_A = -(r_1+r_2+r_4+r_6)$	(1)
$\Re_P = r_7+r_8-r_{11}+r_{12}-r_{13}-r_{14}-r_{15}-r_{16}$	(2)
$\Re_E = r_2+r_9$	(3)
$\Re_Q = r_3+r_5+r_{11}-r_{12}+r_{13}$	(4)
$\Re_M = r_4+r_8+r_{15}$	(5)
$\Re_H = r_6+r_{14}$	(6)
$\Re_D = r_{17}$	(7)
$\Re_C = r_{16}$	(8)

From the rate equations of elementary reactions in Table 3, rates of production of stable molecular species are derived as shown in Table 4. The rate equations in Table 4 include free radical concentrations. When the steady state assumption of free radical concentrations is applied as such to eliminate free radical concentrations, the resulted rate equations are so complicated as they can hardly be applied for furnace design.

1.2 Derivation of stoichiometric rate equations

In order to derive a set of convenient stoichiometric equations and rate equations from the elementary free radical reactions in Table 3, the rates of elementary reactions of hydrogen atom abstraction, r_2, r_4, r_6, r_{14}, r_{15}, and the rate of initiation, r_1, are eliminated from rate equations in Table 4 as followings by the use of the steady state assumption of free radical concentrations.

The steady state of free radicals can be expressed by using matrix form as follow.

	r_1	r_2	r_4	r_6	r_{14}	r_{15}		
$C_3H_7\cdot$	0	1	1	1	0	0	$r_5+r_7+r_8$	(1)
$C_3H_5\cdot$	0	0	0	0	1	1	$r_{16}+r_{17}$	(2)
$C_2H_5\cdot$	1	−1	0	0	0	0	r_3-r_{13}	(3)
$CH_3\cdot$	1	0	−1	0	0	−1	$-r_5+r_8+2r_9-r_{11}+r_{12}+r_{13}+r_{17}$	(4)
$H\cdot$	0	0	0	−1	−1	0	$-r_3-r_7+r_{11}-r_{12}-r_{16}$	(5)
[(1)+(2)+(3)+(4)+(5)]/2								
	1	0	0	0	0	0	$r_8+r_9+r_{17}$	(6)

The matrix may be transformed as follow.

	r_1	r_2	r_4	r_6	r_{14}	r_{15}	
(1)+(6)	1	1	1	1	0	0	$r_5+r_7+2r_8+r_9+r_{17}$
−(2)	0	0	0	0	−1	−1	$-r_{16}-r_{17}$
−(3)+(6)	0	1	0	0	0	0	$-r_3+r_8+r_9+r_{13}+r_{17}$
−(4)+(6)	0	0	1	0	0	1	$r_5-r_9+r_{11}-r_{12}-r_{13}$
−(5)	0	0	0	1	1	0	$r_3+r_7-r_{11}+r_{12}+r_{16}$

Then, the rate equations in Table 5 are obtained by substituting these rerations, respectively, in the rate equations in Table 4.

Now, if the pyrolysis reaction of propane is expressed by the stoichiometric equations in the first column of Table 6, the rates of production of molecular species can be expressed as shown in Table 7, using the rate expressions in the second column of Table 6. From Tables 5 and 7, we find the following correspondences.

TABLE 5. Transformed Rate Equations of Production of Stable Molecular Species

$\Re_A=-(r_5+r_7+2r_8+r_9+r_{17})$	(1)
$\Re_P=r_7+r_8-r_{11}+r_{12}-r_{13}-2r_{16}-r_{17}$	(2)
$\Re_E=-r_3+r_8+2r_9+r_{13}+r_{17}$	(3)
$\Re_Q=r_3+r_5+r_{11}-r_{12}+r_{13}$	(4)
$\Re_M=r_5+r_8-r_9+r_{11}-r_{12}-r_{13}$	(5)
$\Re_H=r_3+r_7-r_{11}+r_{12}+r_{16}$	(6)
$\Re_D=r_{17}$	(7)
$\Re_C=r_{16}$	(8)

$$r_a=r_8,\ r_b=r_9,\ r_c=r_3,\ r_d=r_5,\ r_e=r_7,$$
$$r_f=r_{17},\ r_h=r_{11},\ r_i=r_{12},\ r_j=r_{13},$$
$$r_k=r_{16}$$

In view of these correspondences, the rate expressions in the third column of Table 6 are obtained.

Now, as these rate expressions

TABLE 6. Stoichiometric Equations and Conjugate Rate Equations of Propane Pyrolysis

Stoichiometric equation		Rate equation		
low conversion level:				
initiation and termination step				
$2C_3H_8\rightarrow C_3H_6+C_2H_6+CH_4$	r_a	$k_8C_A\cdot C_M\cdot$	$k_aC_A^n$	(8)
$C_3H_8+CH_4\rightarrow 2C_2H_6$	r_b	$k_9C_M^2\cdot$	$k_bC_A^n$	(9)
propagation step				
$C_2H_6\rightarrow C_2H_4+H_2$	r_c	$k_3C_E\cdot$	$k_cC_A^n$	(3)
$C_3H_8\rightarrow C_2H_4+CH_4$	r_d	$k_5C_A\cdot$	$k_dC_A^n$	(5)
$C_3H_8\rightarrow C_3H_6+H_2$	r_e	$k_7C_A\cdot$	$k_eC_A^n$	(7)
high conversion level:				
initiation and termination step				
$C_3H_8+C_3H_6\rightarrow C_4H_8+C_2H_6$	r_f	$k_{17}C_P\cdot C_M\cdot$	$k_fC_A^n$	(17)
propagation step				
$C_3H_6+H_2\rightarrow C_2H_4+CH_4$	r_h	$k_{11}C_PC_H\cdot$	$k_hC_PC_A^{n-1}$	(11)
$C_2H_4+CH_4\rightarrow C_3H_6+H_2$	r_i	$k_{12}C_QC_M\cdot$	$k_iC_QC_A^{n-1}$	(12)
$C_3H_6+CH_4\rightarrow C_2H_6+C_2H_4$	r_j	$k_{13}C_PC_M\cdot$	$k_jC_PC_A^{n-1}$	(13)
$2C_3H_6\rightarrow$ polymer$+H_2$	r_k	$k_{16}C_PC_P\cdot$	$k_kC_PC_A^{n-1}$	(16)

still include free radical concentrations, the following simplifying approximations are introduced. Assuming the contributions of the initiation and termination reactions for overall process are much less important than the propagation reactions, and assuming the rate of propane disappearance is approximated as n-th power of propane concentration, we obtain the following relations.

TABLE 7. Rate of Production of Stable Molecular Species for Stoichiometric Equations

$\Re_A = -(2r_a + r_b + r_d + r_e + r_f)$	(1)
$\Re_P = r_a + r_e - r_f - r_h + r_i - r_j - 2r_k$	(2)
$\Re_E = r_a + 2r_b - r_c + r_f + r_j$	(3)
$\Re_Q = r_c + r_d + r_h - r_i + r_j$	(4)
$\Re_M = r_a - r_b + r_d + r_h - r_i - r_j$	(5)
$\Re_H = r_c + r_e - r_h + r_i + r_k$	(6)
$\Re_D = r_f$	(7)
$\Re_C = r_k$	(8)

From Eq. (1) in Table 5

$$-\Re_A = k_{t,n}C_A^n = k_4 C_A C_{M\cdot} + k_6 C_A C_{H\cdot}$$

and from Eq. (1) in Table 7 $-\Re_A = k_{t,n}C_A^n = k_5 C_{A\cdot} + k_7 C_{A\cdot}$.

Then, we get $C_{M\cdot} \propto C_A^{n-1}$, $C_{H\cdot} \propto C_A^{n-1}$, $C_{A\cdot} \propto C_A^n$.

Applying these relations, the reactions (5), (7), (11), (12), and (13) in Table 6 are expressed as n-th order reactions. As an additional approximation, the rates of reactions (8), (9), (3), (17), and (16) are expressed by n-th power equations of molecular concentrations, because those reactions are less important than reactions (5) and (7). Then, we obtain the rate equations in the last column in Table 6.

Laidler *et al.*[24] showed that the reaction (8) in Table 3 was less important than the reaction (9) for such higher temperature and lower pressure as our present experiments. Therefore, we can neglect the reaction (8) in Table 6. Our experiments showed that mixing of propylene in propane increased ethylene and methane production, while mixing of ethylene showed no effect. Thus, considering $r_i \ll r_h$ and the addition reactions of methyl radical are less important than the addition reactions of hydrogen atom, we neglected the reactions (12) and (13) in Table 6. The stoichiometric rate equations in Table 7 are then expressed in terms of measurable numbers of the moles of j-th compornents, N_j, as shown in Table 8, where j=A, P, E, Q, M, and H.

TABLE 8. Rate Equations in Terms of N_j

$-dN_A/d\theta = N_{A0}(dX_A/d\theta)$	
$= (k_b + k_d + k_e + k_f) N_A^n V^{1-n}$	(1)
$dN_P/d\theta = \{(k_e - k_f) - (k_h + 2k_k) N_P/N_A\} N_A^n V^{1-n}$	(2)
$dN_E/d\theta = (2k_b - k_c + k_f) N_A^n V^{1-n}$	(3)
$dN_Q/d\theta = \{(k_c + k_d) + k_h N_P/N_A\} N_A^n V^{1-n}$	(4)
$dN_M/d\theta = \{(-k_b + k_d) + k_h N_P/N_A\} N_A^n V^{1-n}$	(5)
$dN_H/d\theta = \{(k_c + k_e) - (k_h - k_k) N_P/N_A\} N_A^n V^{1-n}$	(6)

1.3 Discussions of stoichiometric rate equations

Mixing of propylene in propane acts as an inhibitior for the initial rates of propane pyrolysis as reported by Kershenbaum *et al.*[13] The rate equations in Table 8 obtained from Tables 3 and 6 do not illustrate the inhibitory action of

propylene. Taking into consideration that the hot free radicals can be deactivated by collision with molecules, the free radical reactions (10) ~ (13) in Table 3 are replaced by the reactions (10 a) ~ (13 a) in Table 9 and the stoichiometric equations (11) ~ (13) in Table 7 are replaced by the equations (10 a) ~ (13 a) in Table 9. Then, the stoichiometric rate equations in Table 8 are reduced to the equations in Table 10. They can illustrate the inhibitory action of propylene.

The stoichiometric rate equations for pyrolysis of heavy hydrocarbons are complicated. They might be obtained by combinning stoichiometric rate equations for pyrolysis of each one of primary product hydrocarbons, as shown by Kunii *et al.*[19] for *n*-hexane pyrolysis and by Tominaga *et al.*[45] for pyrolysis of *n*-heptane-hydrogen mixtures. However, rate constants obtained independently for lower hydrocarbons do not satisfy experimental results on higher hydrocarbon. In the original rate expresions for the stoichiometric reactions include concentrations of free radicals as in Tables 6 and 9, and the approximations to eliminate free radical concentrations may differ according with the species of feed hydrocarbon.

Amano *et al.*[1] showed that the rate of reaction between propylene and hydrogen was first-order for each of propylene and hydrogen atom concentration in accord with the equations (11) and (14) in Table 3. But, the rate in propylene-hydrogen mixtures was one-half order for hydrogen molecule. Because of the high concentration of hydrogen molecule, most of the hydrogen atom may be produced from the hydrogen molecules by hydrogen atom abstraction reactions with methyl or

TABLE 9. Replacements of Propagation Steps in Tables 3 and 6

Reaction	Rate equation	
elementary free radical reaction:		
$H\cdot + C_2H_4 \rightarrow C_2H_5\cdot$	$r_{10a} = k_{10a} C_Q C_{H\cdot}$	(10 *a*)
$H\cdot C_3H_6 \rightarrow C_3H_7\cdot$	$r_{11a} = k_{11a} C_P C_{H\cdot}$	(11 *a*)
$CH_3\cdot + C_2H_4 \rightarrow C_3H_7\cdot$	$r_{12a} = k_{12a} C_Q C_{M\cdot}$	(12 *a*)
$CH_3\cdot + C_3H_6 \rightarrow C_4H_9\cdot$	$r_{13a} = k_{13a} C_P C_{M\cdot}$	(13 *a*)
$C_4H_9\cdot + C_3H_8 \rightarrow C_4H_{10} + C_3H_7\cdot$	$r_{13b} = k_{13b} C_A C_{B\cdot}$	(13 *b*)
stoichiometric equation:		
$C_2H_4 + H_2 \rightarrow C_2H_6$	$r_{ga} \quad k_{10a} C_Q C_{H\cdot} \quad k_{ga} C_Q C_A^{n-1}$	(10 *a*)
$C_3H_6 + H_2 \rightarrow C_3H_8$	$r_{ha} \quad k_{11a} C_P C_{H\cdot} \quad k_{ha} C_P C_A^{n-1}$	(11 *a*)
$C_2H_4 + CH_4 \rightarrow C_3H_8$	$r_{ia} \quad k_{12a} C_Q C_{M\cdot} \quad k_{ia} C_Q C_A^{n-1}$	(12 *a*)
$C_3H_6 + CH_4 \rightarrow C_4H_{10}$	$r_{ja} \quad k_{13a} C_P C_{M\cdot} \quad k_{ja} C_P C_A^{n-1}$	(13 *a*)

TABLE 10. Modified Rate Equations

$$-dN_A/d\theta = \{(k_b + k_d + k_e + k_f) - k_{ha} N_P/N_A\} N_A^n V^{1-n} \quad (1)$$

$$dN_P/d\theta = \{(k_e - k_f) - (k_{ha} + 2k_k) N_P/N_A\} N_A^n V^{1-n} \quad (2)$$

$$dN_E/d\theta = (2k_b - k_c + k_f) N_A^n V^{1-n} \quad (3)$$

$$dN_Q/d\theta = (k_c + k_d) N_A^n V^{1-n} \quad (4)$$

$$dN_M/d\theta = (-k_b + k_d) N_A^n V^{1-n} \quad (5)$$

$$dN_H/d\theta = \{(k_c + k_e) - (k_{ha} - k_k) N_P/N_A\} N_A^n V^{1-n} \quad (6)$$

allyl radicals. When pure propane and pure propylene, respectively, is used as feed, the hydrogen atom is produced by the decomposition of propyl radical and the polymerization as shown by reactions (7) and (16) in Table 3. Then, the hydrogen atom concentration can be more satisfactorily approximated by the use of propane or propylene concentration than hydrogen concentration.

Investigations as shown above show that the approximation procedures of free radical concentrations in rate equations to stoichiometric equations may differ according with species of feed hydrocarbon. The rate constants of stoichiometric rate equations should be estimated for each feed hydrocarbon.

2. Experimental Results of Propane Pyrolysis[14]

2.1 Experimental methods

Fig. 1 illustrates the apparatus used in the pyrolysis of propane. The reactor is made from quartz tube of 1.70 cm I.D. and has four sections of 16.5 cm length (volume of one section=37.5 cc), each with sampling tap of 0.60 cm I.D. and thermocouple well. Chromel vs. alumel thermocouples of 0.3 mm dia. were inserted in the thermocouple wells to the center of the reactor. Each section has a electric heating furnace and the temperature is controlled manually by the use of slidacs.

Commercially available pure propane in bomb has a purity over 98%. Impurities are ethane and a small quantity of butane. It used as feed with no purification. After passing through pressure and flow controller, the flow rate was measured by olifice flow meter and flowed into preheater. Water from head tank was flowed through controller and evaporater, and was superheated with preheater. The propane and steam were mixed at the entrance of the reactor. Sample for gas chromatographic analyse was taken out from each of the sampling taps by a rate of 2 cc/sec, so the quenching time is less than 0.1 sec.

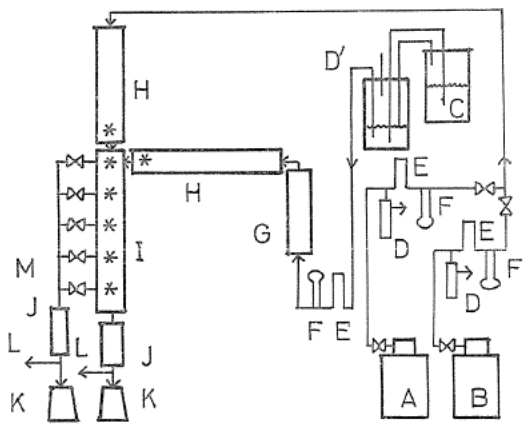

FIG. 1. Schematic diagram of propane pyrolysis apparatus.
A: propane, B: propylene, C: distilled water, D: pressure controller, D': head controller, E: flow controller, F: olifice flow meter, G: evaporater, H: preheater, I: reactor, J: condenser, K: liquid separator, G: gas outlet, M: sampling branch, *: thermocouples.

Molar compositions of gaseous products, hydrogen, methane, ethane, ethylene, propylene, and the non-reacted propane, were measured by gas chromatography. No detectable C_4-hydrocarbons were observed in our experiments. The column used was 4 m of activated alumina with 1% squalane at 45°C, and the carrier gas was nitrogen by 20 cc/min.

2.2 Product distribution

Total 66 runs were tested for ranges of feed rate of propane from 10 to 30 mol/hr, molar ratio of steam to propane from 5 to 10, and temperature between 700 and 750°C. Samples from each of four section of the reactor were analyzed. The mean atomic composition of polymers, *i.e.*, components other than gaseous products detected by gas chromatography was assumed as C_6H_{10}, in view of the mechanism proposed by Tominaga *et al.*[44] From the molar compositions of gaseous products and the atomic composition of polymers, the moles of j-th components based on 100 moles of feed propane, N_j (j=A, P, E, Q, M, and H), and the expansion factor of the reacting gas, ε_A, were calculated by the use of mass balances of C and H atom. The plots of N_j vs. conversion of propane, X_A, are shown in Figs. 2-1 and 2-2. The solid lines in Figs. 2-1 and 2-2 are the relations calculated as shown latter. Propylene was increased at a lower temperature, 650°C, and ethane was increased for lower molar ratios of steam to propane than 5.

In order to investigate effects of secondary reactions at high conversion level, pyrolysis of each one of hydrocarbons in gaseous products and their mixtures with propane were examined. The conversion of methane was small at our experimental conditions, and its secondary reactions could be neglected. The conversion of ethane, ethylene and propylene were large and the secondary reactions must be taken into consideration for these products. However, product distributions of propane pyrolysis with addition of light hydrocarbon, except propylene, in a small quantity agreed with that of pure propane pyrolysis except the added quantity of the hydrocarbon. Thus, the addition of ethane and ethylene

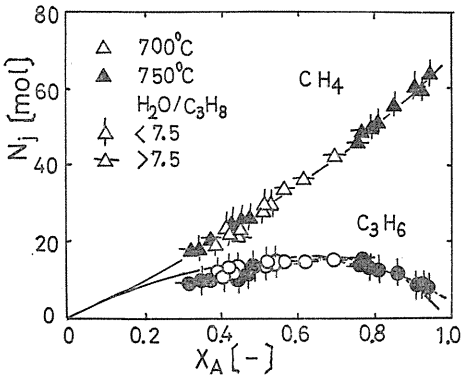

FIG. 2-1. Product distributions for propane pyrolysis (1).
solid line: Table 10, dotted line: Table 8 (deviations from Table 10 only are shown).

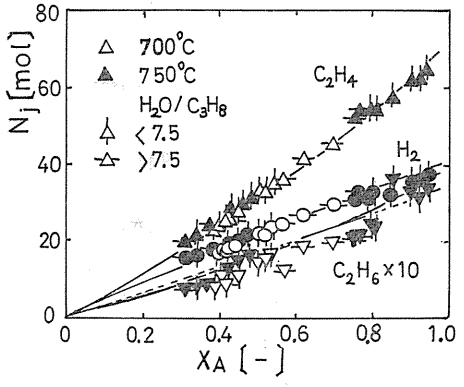

FIG. 2-2. Product distributions for propane pyrolysis (2).
solid line: Table 10, dotted line: Table 8 (deviations from Table 10 only are shown).

in small quantity does not effect the products distribution of propane pyrolysis, while the addition of propylene increase production of ethylene, methane, and coke.

2.3 Rate of propane disappearance

The conversion of propane, X_A, and the expansion factor of the reaction, ε_A, are defined by

$$X_A = (100 - N_A)/100, \qquad \varepsilon_A = (N_t - N_{t0})/100\,X_A$$

Then, the concentration of propane and its rate of disappearance, respectively, are given by

$$C_A = N_A/V = 100\,(1 - X_A)P/N_tRT = (1 - X_A)P/(\varepsilon_A X_A + N_{t0}/100)RT \tag{1}$$

$$-\Re_A = -(1/V)(dN_A/d\theta) = (100\,F_{t0}/37.5\,N_{t0})(dX_A/ds) \tag{2}$$

where, the reaction time, θ, is replaced by position variable, s, represented by the fractional number of the section length of reactor, l, as given by

$$d\theta = [37.5\,P/(F_{t0}N_t/N_{t0})RT]\,ds$$

The values dX_A/ds in Eq. (2) is calculated by numerical differentiations of the relations of conversion of propane vs. section number of the sampling tap.

The rate of propane disappearance is approximated by n-th power equation as mensioned earlier.

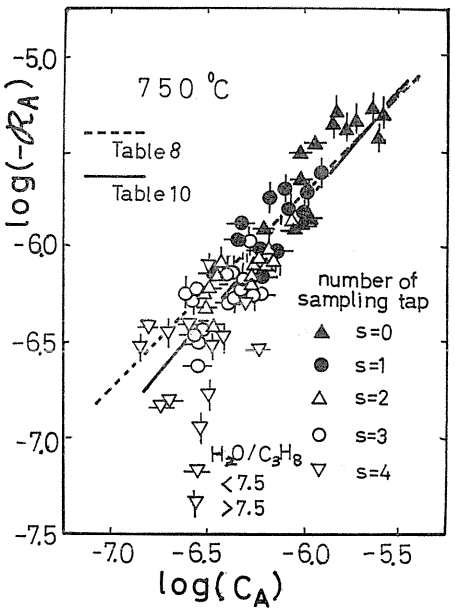

FIG. 3. Comparisons of observed and calculated rate of propane disappearance.

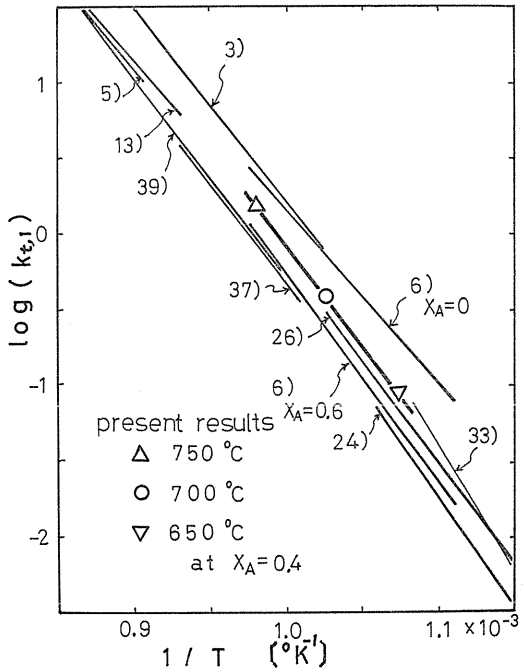

FIG. 4. Arrhenius plots of first-order rate constant of propane disappearance.

$$-\Re_A = k_{t,n} C_A^n \tag{3}$$

The order of reaction, n, obtained experimentary by plotting $\log(-\Re_A)$ vs. $\log C_A$ was distributed between 1.0~1.4 at 650~750°C. The plots of $\log(-\Re_A)$ vs. $\log C_A$ at 750°C are shown in Fig. 3. The solid and dotted lines in Fig. 3 are the relations calculated as shown latter. Assuming first-order, the rate constant, $k_{t,1}$, was calculated for each run. Arrenius plot of the rate constant is shown in Fig. 4. Fig. 4 also contains results from other investigatiors for reference. The heavy solid line in Fig. 4 is the results at $X_A = 0.4$. From this line we obtaine the rate equation as follow.

$$-\Re_A = 6.04 \times 10^{12} \left[\exp\left(-58900/RT\right)\right] C_A \qquad \text{mol}\cdot\text{cc}^{-1}\cdot\text{sec}^{-1} \tag{4}$$

The influences of mixing of small quantities of each one of product species to feed propane on the reaction rate are not detectable except propylene. The latter shows an inhibitive action, especially by an initial small quantity.

2.4 Analog simulation of the reaction

As are shown in Fig. 2, the mole numbers of pyrolysis products, N_j, show good correlations with the conversion of propane, X_A, for the experimental ranges of 700 and 750°C and molar ratios of steam to propane from 5 to 10. Thus, by the simulation of the experimental results on N_j vs. X_A to these relations given by eliminating θ from the rate equations in Tables 8 and 10, the relative values of rate parameters, k_p ($p = b, c, d, e, f, h, ha, k$), were obtained independent of absolute rates of reactions. Then, these parameters can be reduced to absolute values by the use of the rate of propane disappearance given by Eq. (4). The relative values of rate parameters obtained by analog simulation are shown in Table 11. The calculated relations of N_j vs. X_A by the use of those parameter values are shown by solid and dotted lines in Fig. 2. They represent fairly well the experimental points.

TABLE 11. Relative Values of Rate Parameters Obtained by Analog Simulation

k_p in Table 8:						
k_b	k_c	k_d	k_e	k_f	k_h	k_k
0.046	0.040	1.00	0.82	0.013	0.80	0.56
k_p in Table 10:						
k_b	k_c	k_d	k_e	k_f	k_{ha}	k_k
0.035	0.031	0.096	0.78	0.011	1.00	0.39

2.5 Experiment with feed containning propylene

The addition of propylene in feed propane shows an inhibitive action by an initial small quantity on the rate of propane disappearnce, and increases production of ethylene, methane, and coke. The plots of N_j vs. N_A for pyrolysis of propane containning 10, 20, and 40% propylene, respectively, are shown in Figs. 5-1 and 5-2. Product distributions of pyrolysis of propane mixed with propylene were calculated from the rate equations in Table 10, applying values of rate parame-

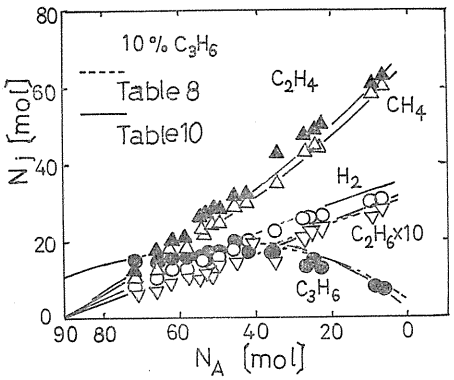

FIG. 5-1. Product distributions for pyrolysis of propane mixed with 10% propylene.

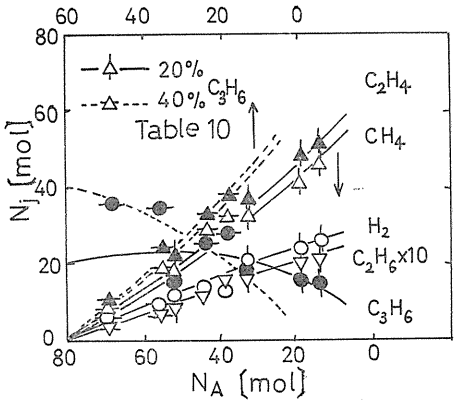

FIG. 5-2. Product distributions for pyrolysis of propane with 20 and 40% propylene.

ters in Table 11. The results are shown by solid and dotted lines in Figs. 5-1 and 5-2. They agree well with experimental points. The rate equations in Table 10 is superior than the rate equations in Table 8 in that the former can illustrate inhibitory action of propylene. However, the rate equations in Table 10 can not yet illustrate the inhibitory action of initial small quantity of propylene. A method to represent the free radical concentrations in the rate equations in Tables 6 and 9 by expressions containing only measurable molecular concentrations and have denominator of inhibitory molecular concentrations was also examined. But, the analysis of free radical concentrations by such method is too complicated for our present purpose. Therefore, the stoichiometric rate equations derivated in Table 10 were applied for further investigations.

3. Estimation of Optimum Parameters in Stoichiometric Rate Equations[16)17)]

3.1 Introduction

Investigations of the estimation of parameters in rate equations were reviewed recently by Morita *et al.*[30)31)] Although, there are many publications in this field, experimental investigations are rather rare, especially for multi-response rate processes.

In the present report, three kinds of Gauss method are first compared each other in their efficiencies to evaluate optimum values of parameters in the rate equations in Table 10. The three methods are: application of Gauss method to integral rate, *i.e.*, the moles of product species, N_j, application to relative rates of production of product species to the conversion of propane, dN_j/dX_A, and application to the sum of squares of residuals of moles of product species, $\delta = \sum_j (N_{j,\mathrm{obs}} - N_{j,\mathrm{calc}})^2$. Secondly, these results are compared with steepest descent method and Marquardt method. Detailed discussions of the step size in the steepest descent method and weighting factor in the Marquardt method are given.

3.2 Methods of estimation

3.2.1 Gauss method applied to integral rates of reactions (Method A) In this method, the sum of squares of residuals is $S_A = \sum_i \sum_j (N_{j,\mathrm{obs}} - N_{j,\mathrm{calc}})_i^2$, where $N_{j,\mathrm{calc}}$ is the mole number of j-th compornent calculated by numerical integration of the rate equations in Table 10 applying appropriate initial values of rate parameters, $k_{p,0}$. To minimize S_A, we have $\partial S_A/\partial(\Delta k_p)=0$, and obtain the following normal equations.

$$\sum_i \sum_j \sum_p \left[\left(\frac{\partial N_j}{\partial k_p}\right)_0 \left(\frac{\partial N_j}{\partial k_q}\right)_0 (\Delta k_p) \right]_i = \sum_i \sum_j \left[(N_{j,\mathrm{obs}} - N_{j,0}) \left(\frac{\partial N_j}{\partial k_q}\right)_0 \right]_i \qquad (5)$$

Starting from the initial values of parameters as determined by analog simulation and the initial values of moles of component, $N_{j,0}$, calculated by applying the initial parameter values to the rate equations, corrections for parameters, Δk_p, are obtained by solving the linear simultaneous equations (5) by digital computer. These corrections are added to initial values of rate parameters. The corrected values of parameters are used as the initial values of second iteration and so on, until the sum of squares of residuals reach a specified small value, and the optimum values of rate parameters are obtained.

In the derivation of the normal equations (5), we have not taken into consideration of the weights of responses. When the variances differe for each responses, we need to use weighting factors associated with observed values of responses, $N_{j,\mathrm{obs}}$. The weighting factors may be given by inversely proportional values of variances. However, for such complex reactions as the propane pyrolysis, the variances in experimental values of molar concentrations can not be obtained, because identical experimental conditions are difficult to be realized. Mezaki *et al.*[29] applied Bayes' function for a complex chemical system with three responses. However, application of the methods becames very difficult for such complex systems as in present report, because the normal equations are six-order simultaneous equations with seven elements. Therefore, we use Eq. (5) as normal equations, assuming the weighting factors are the same for all of components.

In this method, the initial values of rate parameter $k_{p,0}$ are substituted into the rate equations in Table 10, and the $(N_{j,0})_i$ are calculated by applying Runge-Kutta-Gill numerical integration method for every experimental points corresponding to the experimental conversions of propane, setting the time step $\Delta\theta$ as a parameter. During the calculation, we need to evalute $(\partial N_j/\partial k_p)_{0,i}$ for every step of calculations. These values are obtained by evaluating variation in values of N_j, $N_{j,0}+\Delta N_{j,0}$, by the use of variated values of parameters, $k_{p,0}+\Delta k_{p,0}$, and setting $(\partial N_j/\partial k_p)_{0,i} = (\Delta N_j/\Delta k_p)_{0,i}$ for each iteration (see page 78). These calculations are included in the program of computer.

To examine the approach of the calculated values of k_p to the optimum values, the standard deviation, or the variance, of N_j is calculated for every step by

$$\sigma_{Nj} = \left[\sum_i \sum_{j \neq A} (N_{j,\mathrm{obs}} - N_{j,\mathrm{calc}})_i^2 / (J-1)(I-P)\right]^{1/2} \qquad (6)$$

3.2.2 Gauss method applied to differential rates of reactions (Method B) If we eliminate time θ by dividing the rate equations in Table 10 for each compornent

of products by that for propane, we obtaine equations for the relations between the modified rate of reaction, (dN_j/dX_A), and the conversion of propane, X_A. Set the sum of squares of residuals by $S_B = \sum_i \sum_j [(dN_j/dX_A)_{obs} - (dN_j/dX_A)_{calc}]_i^2$. The normal equations for least square calculation are:

$$\sum_i \sum_j \sum_p \{[\partial(dN_j/dX_A)/\partial k_p]_0 [\partial(dN_j/dX_A)/\partial k_q]_0 (\Delta k_p)\}_i = \sum_i \sum_j \{[(dN_j/dX_A)_{obs} - (dN_j/dX_A)_0][\partial(dN_j/dX_A)/\partial k_q]_0\}_i \quad (7)$$

In order to evaluate $(dN_j/dX_A)_{obs,i}$, each of the observed values of moles, $N_{i,obs}$, is expresed by a third-order exponential polynomial with variable X_A, and the derivatives of the polynomial are calculated at the observed points, $X_{A,i}$. These calculations are including in the program of computer.

The standard deviation of dN_j/dX_A is calculated by

$$\sigma_{dN_j/dX_A} = \{\sum_i \sum_{j \neq A} [(dN_j/dX_A)_{obs} - (dN_j/dX_A)_{calc}]_i^2/(J-1)(I-P)\}^{1/2} \quad (8)$$

For the purpose of comparison with method A, σ_{N_j} is also calculated using Eq. (6).

3.2.3 Gauss method applied to the sum of squares of residuals of each run (Method C) The residual of moles of each experimental run is given by $\delta_i = \sum_j (N_{j,obs} - N_{j,calc})_i^2$, and its value is evaluated by

$$\delta_i = \delta_{i,0} + \sum_p [(\partial\delta/\partial k_p)_0 (\Delta k_p)]_i \quad (9)$$

Thus, we have to minimize $S_C = \sum_i \delta_i^2$. This kind of method is applied for ethane pyrolysis by Snow[41]. The normal equations for the least square calculations of the correction for parameters, Δk_p, are

$$\sum_i \sum_p \left[\left(\frac{\partial\delta}{\partial k_p}\right)_0 \left(\frac{\partial\delta}{\partial k_q}\right)_0 (\Delta k_p)\right]_i = -\sum_i \left[\delta \left(\frac{\partial\delta}{\partial k_q}\right)_0\right]_i \quad (10)$$

The standard deviation, δ_{N_j}, is calculated by Eq. (6).

3.2.4 Steepest descent method applied to integral rate of reactions (Method D) Here, we have to find the direction of steepest desent of the sum of squares of residuals, $S_D = \sum_i \sum_j (N_{j,obs} - N_{j,0})_i^2$ when infinitesimal changes are given to the initial values of rate parameters. Let the direction of the infinitesimal change in k_p is denoted by

$$(dr)^2 = \sum_p (dk_p)^2 \quad (11)$$

Then, the change of S_D is given by

$$dS_D/dr = \sum_p (\partial S_D/\partial k_p)(dk_p/dr) \quad (12)$$

In order to get the direction of minimizing S_D, we have to find the direction to get the most negative value of Eq. (12).

From Eq. (11) we get, $1-\sum_p(\mathrm{d}k_p/\mathrm{d}r)^2=0$, and from Eq. (12) we obtain the following function by using a Lagrange multiplier, λ.

$$\sum_p(\partial S_D/\partial k_p)(\mathrm{d}k_p/\mathrm{d}r)+\lambda[1-\sum_p(\mathrm{d}k_p/\mathrm{d}r)^2] \tag{13}$$

Derivative of function (13) with respect to $\mathrm{d}k_p/\mathrm{d}r$ is set equal to zero.

$$(\partial S_D/\partial k_p)+\lambda(-2\,\mathrm{d}k_p/\mathrm{d}r)=0 \tag{14}$$

Then, the λ is obtained as follow

$$\lambda=\pm(1/2)[\sum_p(\partial S_D/\partial k_p)^2]^{1/2} \tag{15}$$

Substitution into Eq. (14) gives

$$\mathrm{d}k_p/\mathrm{d}r=\pm(\partial S_D/\partial k_p)[\sum_p(\partial S_D/\partial k_p)^2]^{-1/2} \tag{16}$$

Thus, when the step size for correction is denoted by $\Delta r=\lambda_s$, the equations to obtaine corrections for parameters are given as follow.

$$\Delta k_p=-\lambda_s(\partial S_D/\partial k_p)_0/[\sum_p(\partial S_D/\partial k_p)_0^2]^{1/2} \tag{17}$$

The standard deviation, σ_{x_j}, is calculated by the aid of Eq. (6).

3.2.5 Marquardt method applied to integral rate of reactions (Method E) Marquardt[27] modified the steepest descent method with the Gauss method. The normal equations to find Δk_p are given by

$$\sum_p\Big\{\sum_i\sum_j\Big[\Big(\frac{\partial N_j}{\partial k_p}\Big)_0\Big(\frac{\partial N_j}{\partial k_q}\Big)_0\Big]_i+\lambda_L\Big\}(\Delta k_p)=\sum_i\sum_j\Big[(N_{j,\mathrm{obs}}-N_{j,0})\Big(\frac{\partial N_j}{\partial k_q}\Big)_0\Big]_i \tag{18}$$

where, $\lambda_L=0$ for $q\neq p$. The λ_L is a weighting factor, and $\lambda_L=0$ or ∞ reduces Eq. (18) to Gauss or steepest descent method, respectively.

Ball *et al.*[4] used the following normal equations in places of Eq. (18).

$$\sum_p\Big\{\sum_i\sum_j\Big[\Big(\frac{\partial N_j}{\partial k_p}\Big)_0\Big(\frac{\partial N_j}{\partial k_q}\Big)_0\Big]_i\Big\}(1+\lambda_L)(\Delta k_p)=\sum_i\sum_j\Big[(N_{j,\mathrm{obs}}-N_{j,0})\Big(\frac{\partial N_j}{\partial k_q}\Big)_0\Big]_i \tag{19}$$

where, $\lambda_L=0$ for $q\neq p$. The values of λ_L in Eq. (18) must be changed with the values of $\sum_i\sum_j[(\partial N_j/\partial k_p)_0(\partial N_j/\partial k_q)_0]_i$, while the value λ_L in Eq. (19) is given in relation to a fixed value designated by 1. In the following calculations of the optimum rate parameters, Eq. (19) is applied. The standard deviation is calculated using Eq. (6).

3.3 Calculations of optimum parameters

The optimum values of the rate parameters of the stoichiometric rate equations in Table 10, assuming $n=1$, were calculated by the use of the experimental values of moles of product compoments obtained in Chapter 2 and shown in Fig. 7. The number of chemical species, the number of rate parameters, and the number of experimental points applied for the calculations were $J=6$, $P=7$, and

TABLE 12. Rate Parameters Obtained by Methods A, B and C, after Six Iterations. $k_d=1.000$ (Standard)

k_p	Initial	A	B	C	Initial	A	B	C
k_b	0.036	0.019	0.006	−0.003	0.01	0.019	0.007	−0.026
k_c	0.032	0.076	0.078	0.095	0.01	0.076	0.078	0.099
k_e	0.813	0.715	0.501	0.728	1.0	0.712	0.500	0.784
k_f	0.011	0.076	0.091	0.142	0.01	0.077	0.090	0.190
k_{ha}	1.042	0.909	0.332	0.937	1.0	0.906	0.328	1.292
k_k	0.406	0.336	0.220	0.301	1.0	0.330	0.222	0.295
σ_{N_j}	1.590	1.018	2.596	1.240	5.010	1.023	2.594	1.609
σ_{dN_j/dX_A}	64.68	—	5.69	—	59.63	—	5.62	—

$I=66$, respectively. The optimum values of parameters obtained by the three Gauss methods, A, B, and C, are shown in second to fifth column of Table 12 and the modes of convergency with iteration numbers are plotted in Figs. 6-1 ~ 6-3. The moles of product components calculated from rate equations in Table 10 by applying the parameter values obtained by method A, which gives a minimum values of variance, are shown by solid lines in Fig. 7. We see from Figs. 6-1 ~ 6-3 that the calculated values of rate parameters become almost at constants after third iteration for all of the three methods, although the final values differ each other.

The HITAC 5020 digital computer in Tokyo University was used for the calculations. The times of calculations were five minutes for methods A and C, and two minutes for method B, each including the time of calculations of σ_{N_j}. The time step was $\Delta\theta=0.001$ and the width of variation of $k_{p,0}$ to calculate the gradients $(\Delta N_j/\Delta k_p)_{0,i}$ and $(\Delta\hat{\sigma}/\Delta k_p)_{0,i}$ in Eqs. (5) and (10), was 20%, *i.e.*, $\Delta k_{p,0}=0.2\,k_{p,0}$.

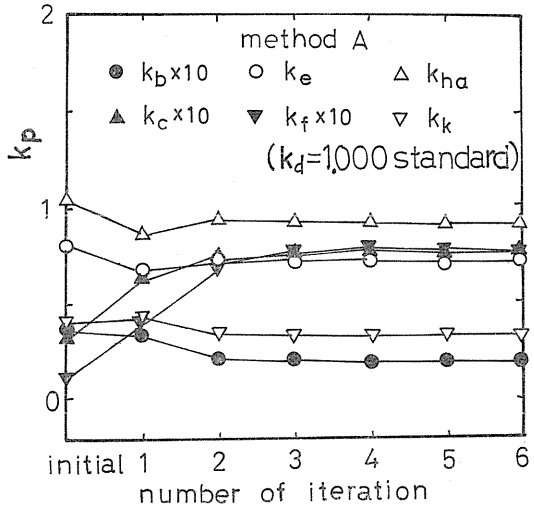

FIG. 6-1. Changes of parameter valus with number of iteration (method A).

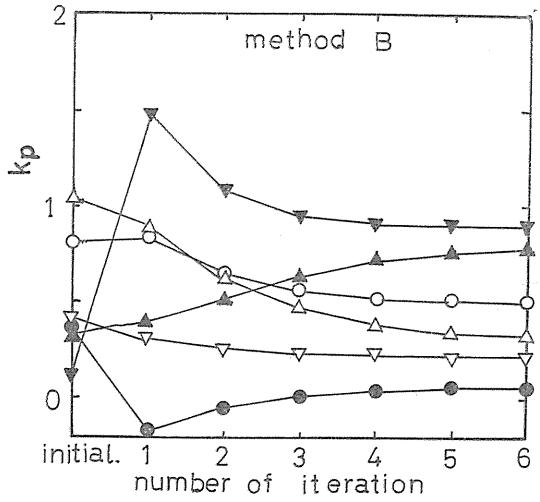

FIG. 6-2. Changes of parameter values with number of iteration (method B). Key points are the same as in Fig. 6-1.

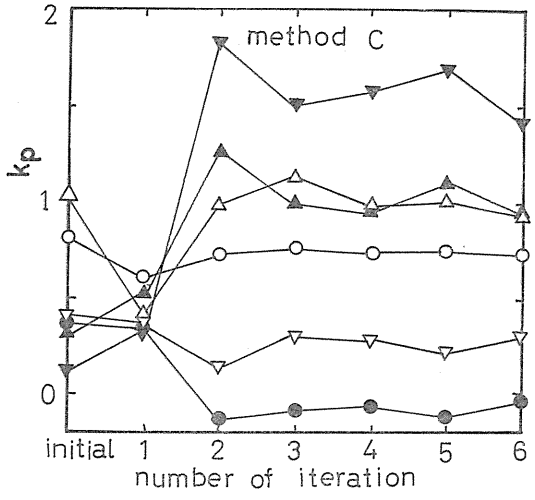

FIG. 6-3. Changes of parameter values with number of iteration (method C). Key points are the same as in Fig. 6-1.

In order to examine the effect of initial values to the estimated optimum values of the rate parameters, we tried the calculations with different initial values. Because the values of k_b, k_c, and k_f, which are in connection with the reactions of initiation and termination steps, are expected to be much smaller than the other parameters, we set the initial values of these parameters as 1/100 of other parameters. The results of estimation were shown in seventh to ninth column in Table 12. The values obtained by methods A and B agree well with those obtained above, while the values obtained by method C show some variations, which may be attributed to the vibrational character of method C.

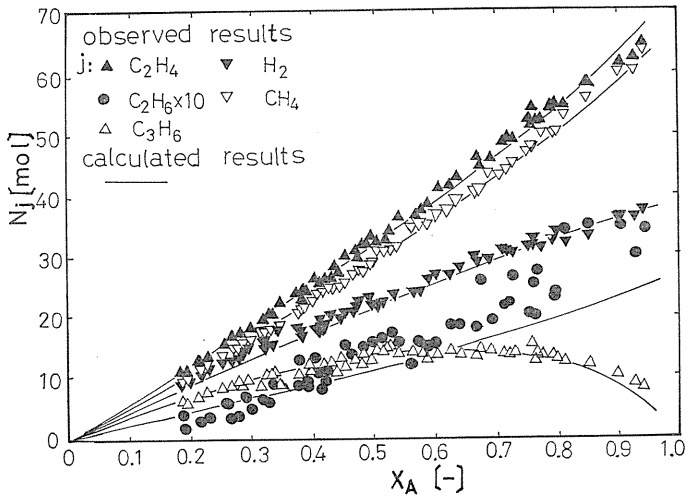

FIG. 7. Observed and calculated distributions of products for propane pyrolysis.

TABLE 13. Rate Parameters Obtained by Method D and E, after Six Iterations. k_a=1.000 (Standard)

method D:

k_p	Initial	λ_S 0.2	λ_S 0.02	Initial	λ_S 0.2	λ_S 0.02
k_b	0.036	0.093	0.034	0.01	−0.061	−0.006
k_c	0.032	0.048	0.034	0.01	0.124	0.026
k_e	0.813	0.689	0.748	1.0	0.567	0.884
k_f	0.011	0.139	0.033	0.01	0.116	0.067
k_{ha}	1.042	1.022	1.062	0.01	0.101	0.038
k_k	0.406	0.410	0.415	0.01	0.127	0.047
σ_{N_j}	1.590	4.960	1.252	9.379	3.935	6.898

method E:

k_p	Initial	λ_L 1.0	λ_L 0.2	Initial	λ_L 1.0	λ_L 0.2
k_b	0.036	0.034	0.026	0.01	0.019	0.021
k_c	0.032	0.051	0.068	0.01	0.069	0.077
k_e	0.813	0.727	0.712	1.0	0.651	0.705
k_f	0.011	0.030	0.058	0.01	0.068	0.074
k_{ha}	1.042	0.997	0.912	0.01	0.593	0.867
k_k	0.406	0.445	0.376	0.01	0.353	0.339
σ_{N_j}	1.590	1.088	1.058	9.379	1.121	1.021

Other initial values were also tried for method A and C. Here, the initial values were assumed to be 1/100, for all parameters except k_d and k_e, which were connected to the main reactions of the propagation steps. Method A showed overflow, while method C showed stability but did not converge to such a small values of variance as obtained above.

The optimum values of parameters obtained by method D and E are shown in Table 13. Two sets of initial values were tested, *i.e.*, the values of k_p in Table 11 evaluated by analog simulations and those mentioned in last section, with which the method A resulted over flow. The step sizes in method D were λ_s= 0.2 and 0.02 and the weighting factors in method E were λ_L=1.0 and 0.2. The times of calculations were three and one half minutes for method D and five minutes for method E. The decreases of the standard deviations with increase in iteration number for methods D and E are shown in Fig. 8.

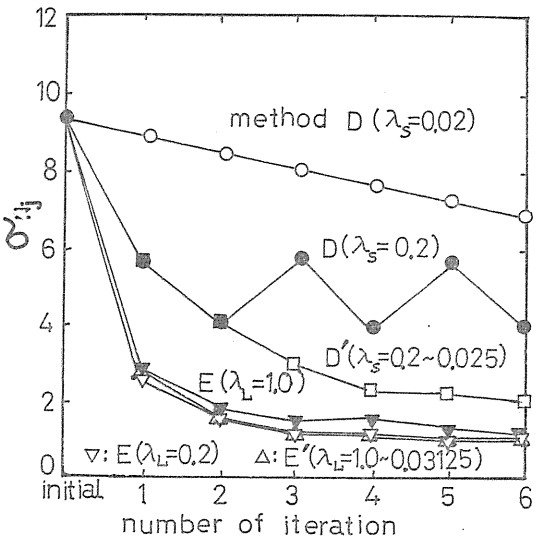

FIG. 8. Changes of standard deviations with number of iteration.

3.4 Discussions of the results

Method A has a superiority over others in that it gives the smallest variance when good initial values of rate patameters are available by some ways such as analog simulation. Method B has an advantage over method A in the short time of calculation. But, in spite of the monotonous decrease of the variance of dN_j/dX_A accompanied with increase in number of iteration, the variance of N_j reaches to a minimum and then increase with the number of iteration. The values of parameters at the minimum point differ remarkably from the values obtained by method A. These irregularities may be attributed to the errors in the differertiation of experimental values of N_j vs. X_A to get dN_j/dX_A. Method C are stable for large fluctuations of initial values of parameters. But, this method results vibrating values as seen from Fig. 6-3 and the variance is large. These irregularities may be attributed to the high correlations between N_j's, because

in method C, $(\partial\delta/\partial k_p)_{0,i}$ are evaluated in connection of the sum of all components in every run, while, in method A, $(\partial N_j/\partial k_p)_{0,i}$ are evaluated for each component in every run.

Method D also gives vibrating values if the step size λ_S is large and the convergence is limited as seen from Fig. 8. In such a case, we need to decrease the step size according to advances of iterations. In method E, small values of the weighting factor λ_L bring the method close to method A, and becomes unstable if the initial values are unsuitable. Thus, we need to decrease the weighting factor gradually according to advances of the iterations. An example of adjustment of the weighting factor was shown by Marquardt[27]. But, for such complex system as our present rate equations which need $(P+1)$-mal numerical integration for one iteration, the adjustment of the step size in method D or the weighting factor in method E is too time-consuming, and we are obliged to use simple methods.

In another calculation by the method D with a starting value of $\lambda_S=0.2$, the step size was decreased in succesion to one half of the preceeding value whenever the standard deviation exceeded that of former calculation (called method D'). Similarly, in method E with a starting value of $\lambda_L=1.0$, the weighting factor was decreased in succesion to one half of the preceeding values for every iteration (call method E'). The parameter values obtained by methods D' and E' are shown in Table 14. The standard deviations for methods D' and E', respectively, are superior to methods D and E.

In comparison of method D' with method E', the former is less advantageous in that it does not converge to same values of parameters for different initial values and the standard deviations is also larger than that for method E'. The steepest descent method has a profit of stability for deviations in initial values of rate parameters, but it needs too much time to achieve covergence. Therefore, this method can not be applied for such cases as our present problem.

Method C was stable, but gave vibrating parameter values. Therefore, we tried a method (called method C') to multiply a factor λ_C for all of Δk_p. Starting with $\lambda_C=1.0$, the step size was decreased in succesion to one half of preceeding value whenever the standard deviation exceeded that of preceding calculation. Method C' was superior to method C, because the former gave no vibrating

TABLE 14. Rate Parameters Obtained by Methods D' and E', after Six Iterations. $k_a=1.000$ (Standard)

	methods:	D'	E'		D'	E'
k_p	Initial	λ_S 0.2～0.0125	λ_L 1.0～0.03125	Initial	λ_S 0.2～0.025	λ_L 1.0～0.03125
k_b	0.036	0.027	0.023	0.01	−0.020	0.019
k_c	0.032	0.038	0.073	0.01	0.084	0.077
k_e	0.813	0.748	0.713	1.0	0.583	0.713
k_f	0.011	0.028	0.068	0.01	0.142	0.076
k_{ha}	1.042	1.061	0.911	0.01	0.105	0.900
k_k	0.406	0.414	0.355	0.01	0.126	0.337
σ_{Nj}	1.590	1.180	1.023	9.379	2.035	1.020

parameter values and has less standard deviations, but not converged to small value such as obtained by method E′.

In conclusion, when good initial values of rate parameters can not be obtained, Marquardt method with decreasing weighting factor for every iterations as like in method E′, and thus approaching to Gauss method, may be the best way, and will be applicable for many kinds of complex problems.

4. Sample Calculation for Designing Tubular Pyrolysis Unit[15]

4.1 Histrical backgrounds

Methods of designing multiple tubular reactors for hydrocarbon pyrolysis were reported by Fair *et al.*[7] and Perkins *et al.*[34] using the results of experiments by Schutt[37]. The former reported a step wise trial and error method assuming temperature and pressure of the reacting gases for tube to tube of the reactor, and the latter used numerical integration method where the incremental increase of the expansion factor was assumed as the same as that of preceding step and, thus, decreased the time of calculation to one fourth of the former. However, these methods used charts of over-all rate constant of reactant disappearance vs. temperature and product distributions vs. conversion.

Several authors reported recently the designing methods applied stoichiometric rate equations and digital and analog computations. Snow *et al.*[32] and Andrews *et al.*[2], respectively, calculated the number of reactor tubes for ethane and butane pyrolysis. However, these methods need stepwise trial and error calculations, setting assumptions on the change of moles, temperature and pressure for each stage.

In our present calculation, an improved method is presented for designing a multiple tubular reactor for propane pyrolysis, where no trial calculation is required except for temperature and pressure, by using the stoichiometric rate equations and optimum parameter values obtained in Chapters 1～3.

4.2 Estimation of number of tubes for pyrolysis reactor

4.2.1 Application of the stoichiometric rate equations Applying the relative values of rate parameters obtained by method A in Table 12 to the stoichiometric rate equations in Table 10, Eqs. (1)～(6) in Table 15 are obtained, assuming $n=1$ and changing time θ in sec to time τ in hr. Eqs. (7)～(9) are added to supplement the reactions of non-measurable components by the gas chromatography. The rate constant k_1 as shown in Eq. (10) in Table 15 was obtained by substituting mean experimental values of $N_P/N_A=0.193$ at $X_A=0.40$ in Eq. (1) in Table 15, compared with rate equation of propane disappearance at $X_A=0.40$, *i.e.* Eq. (4), and changing the time unit into hr.

TABLE 15. Rate Equations Applied for Design of Pyrolysis Furnace

$-dN_A/d\tau=k_1(1.810\,N_A-0.909\,N_P)$	(1)
$dN_P/d\tau=k_1(0.639\,N_A-1.581\,N_P)$	(2)
$dN_E/d\tau=k_1(0.038\,N_A)$	(3)
$dN_Q/d\tau=k_1(1.076\,N_A)$	(4)
$dN_M/d\tau=k_1(0.981\,N_A)$	(5)
$dN_H/d\tau=k_1(0.715\,N_A-0.573\,N_P)$	(6)
$dN_D/d\tau=k_1k_fN_A=k_1(0.076\,N_A)$	(7)
$dN_C/d\tau=k_1k_kN_P=k_1(0.336\,N_P)$	(8)
$dN_S/d\tau=0$	(9)
$k_1=1.33\times10^{16}\exp(-58.9\times10^3/RT)$ hr^{-1}	(10)

4.2.2 Changes of moles and residence time with tube number Average temperature and pressure of gas in n-th tube of the furnace are first assumed in terms of their changes in preceding tube as follow:

$$\overline{T}_n = T_{n-1} + (T_{n-1} - T_{n-2})/2, \qquad \overline{P}_n = P_{n-1} + (P_{n-1} - P_{n-2})/2$$

Here, T_{n-1} and P_{n-1} are temperature and pressure at the exit of $(n-1)$th tube, respectively. Substituting the reaction time and the moles of product components at the exit of $(n-1)$th tube, *i.e.*, τ_{n-1} and $N_{j,n-1}$, as the inlet values to n-th tube in the stoichiometric rate equations in Table 10, the moles of product components at reaction time $\tau_{n-1}+m\Delta\tau (m=1, 2, \ldots)$ are calculated stepwise by Runge-Kutta-Gill numerical integration method. The time increment $\Delta\tau$ is taken as one-hundredth of $\Delta\tau_{n-1}=\tau_{n-1}-\tau_{n-2}$. The volume of gas flowed during the time $m\Delta\tau$ is evaluated by

$$V_m = 0.08205\, m\Delta\tau \overline{F}_m \overline{T}_m / \overline{P}_m \quad \mathrm{m^3} \tag{20}$$

where, $\overline{F}_m=(F_{n-1}+F_m)/2$ is mean molar flow rate in kg-mol/hr, $\overline{T}_m=(T_{n-1}+T_m)/2$ is mean temperature in °K, $\overline{P}_m=(P_{n-1}+P_m)/2$ is mean pressure in atm, and 0.08205 m³·atm/kg-mol·°K is the gas constant. When V_m is less than the volume of one tube, V_{tube}, the stepwise calculation is continued until V_m just exceeds V_{tube}.

The values of τ and N_j at this limitting point are defined as their values at the exit of n-th tube, *i.e.*, τ_n and $N_{j,n}$.

4.2.3 Calculation of gas temperature Mean molar heat capacity of gases and mean enthalpy of reaction in n-th tube, $(\overline{C}_p)_n$ and $(\overline{\Delta H})_n$, are calculated by the methods described latter, assuming mean temperature of the n-th tube, $\overline{T}_n$. By the use of these values, a trial gas temperature at the exit of the n-th tube, T_n^*, is calculated by the following heat balance equation.

$$T_n^* - T_{n-1} = [\pi d' l q / \overline{F}_n (\overline{C}_p)_n] - [(\overline{\Delta H})_n / (\overline{C}_p)_n] \tag{21}$$

where, q [kcal/hr·m²] is the heat flux from the wall. Then, the mean temperature of gas in n-th tube is obtained by $\overline{T}_n^* = (T_n^* + T_{n-1})/2$. When the estimated mean temperature, $\overline{T}_n^*$, deviate from the assumed values, $\overline{T}_n$, the calculation is repeated assuming revised mean temperature by $\overline{T}_n^*$ until the deviation become less than $T_0/200$, and then $T_n = T_n^*$. If T_n exceeds an allowable maximum value, heat supply is decreased by 1000 kcal/hr, *i.e.* to $q-1000$. This procedure is included in the program of computer. But, in our trial calculation shown latter, no such case was appeared.

4.2.4 Calculation of pressure drop Mean molecular weight, mean density, and mean viscosity at n-th tube, $\overline{M}_n$, $\overline{\rho}_n$, and $\overline{\mu}_n$, are calculated as described below. Equivalent length of one tube is given, by using equivalent tube length $75\,d$ for a 180 bent, by[12]

$$L_e = l + 75\, d \tag{22}$$

The estimated values of gas pressure at the exit of the n-th tube, P_n^*, can be obtained using the following equation, which is obtained by substituing Blasius

equation, $f=0.0791\,R_e^{-0.25}$ for tubulent flow, into friction factor, f, in Fanning equation[12].

$$P_{n-1}-P_n^*=3.089\times10^{-13}\left[\frac{(\overline{F}_n\overline{M}_n)^{1.75}}{d^{4.75}}\right]\left(\frac{\bar{\mu}_n^{0.25}}{\bar{\rho}_n}\right)L_e \tag{23}$$

The mean pressure in n-th tube is obtained by $\overline{P}_n^*=(P_n^*+P_{n-1})/2$.

When the calculated value $\overline{P}_n^*$ does not agree with assumed value $\overline{P}_n$, the calculation is repeated by assuming mean pressure by $\overline{P}_n^*$ until the deviation decreases less than $P_0/200$. The final value of P_n^* is set equal to the exit pressure of n-th tube, P_n.

4.2.5 Calculation of wall temperature For the calculation of the wall temperature of reactor tubes, we need information on the rate of coke deposition. As we have no knowledge on it at present, the calculation is proceeded by neglecting the effect of coke. By the use of mean heat conductivity of gases in n-th tube, $(\bar{k}_g)_n$, calculated as described latter, mean Reynolds number and mean Prandtl number in the n-th tube are obtained by

$$(\overline{R}_e)_n=4\,\overline{F}_n\overline{M}_n/\pi d\bar{\mu}_n,\qquad(\overline{P}_r)_n=(\overline{C}_p)_n\bar{\mu}_n/(\bar{k}_g)_n$$

Then, the heat transfer coefficient of gas film, h_n, is calculated by[12]

$$\bar{h}_n=0.023(\overline{R}_e)_n^{0.8}(\overline{P}_r)_n^{1/3}(\bar{k}_g)_n/d\quad\text{kcal/hr}\cdot\text{m}^2\cdot{}^\circ\text{C} \tag{24}$$

From this coefficient and the heat conductivity of wall, $(\bar{k}_w)_n$, the overall heat transfer coefficient at the wall is calculated by

$$\overline{U}_n=1/\{(d'/\bar{h}_nd)+[d'(d'-d)/(\bar{k}_w)_n(d'+d)]\}\quad\text{kcal/hr}\cdot\text{m}^2\cdot{}^\circ\text{C} \tag{25}$$

The mean wall temperature at the n-th tube is then given by $(\overline{T}_w)_n=\overline{T}_n+q/\overline{U}_n$.

4.2.6 Determination of final tube number When the conversion at the exit of n-th tube obtained by $X_{A,n}=(N_{A,0}-N_{A,n})/N_{A,0}$ is less than an allowable minimum conversion, $X_{A,\min}$, the calculations are repeated until $X_{A,n}\geqq X_{A,\min}$.

For this final step, the number of reactor tube and gas pressure are denoted by n_E and P_E. If the restriction conditions $P_{\max}\geqq P_E\geqq P_{\min}$ (where, $P_{\max}$ and $P_{\min}$ are allowable maximum and minimum pressure, respectively, and we set $P_{\max}=P_{\min}+0.3$) are not satisfied, we need to repeat the calculations by setting $P_0=P_0\pm0.1$.

4.3 Design conditions and physical properties

4.3.1 Design conditions Refering to the previous publications, the following design conditions are sellected:

(1) Condition of feed gases

Temperature and pressure: $T_0=338.2$°K, $P_0\leqq5$ atm-abs

Mole numbers and flow rates: $N_{A,0}=100$ kg-mol, $N_{S,0}=20$ kg-mol/100 kg-moles of feed propane, $F_{A,0}=60$, $F_{S,0}=12$ kg-mol/hr.

(2) Conditions for tubes

I.D. and O.D.: $d=0.105$ cm, $d'=0.114$ cm

Equivalent length of one tube including one 180 bent: $L_e=7.3$ m
Volume of one tube: $V_{tube}=(\pi d^2/4)\,l=0.0632$ m^3
Heat flux, and heat supply to one tube: $q=27000$ kcal/hr·m^2, $Q=\pi d'lq=70600$ kcal/hr. Other values are also examined

(3) Conditions of constriction
Gas temperature in tubes: $T_n \leqq T_{max}=1073.2$°K
Gas pressure at final exit: $P_E \geqq P_{min}=1.7$ atm-abs
Conversion at final exit: $X_{A,E} \geqq X_{A,min}=0.65$

4.3.2 Evaluations of pysical properties

(1) Mean molecular weight and mean density:

$$\overline{M}_n=\sum_j M_j \bar{y}_{j,n}, \quad \bar{\rho}_n=\overline{P}_n \overline{M}_n/0.08205\,\overline{T}_n$$

where, $\bar{y}_{j,n}=\overline{N}_{j,n}/\sum_j \overline{N}_{j,n}$: mean mole fraction of component-j, and $\overline{N}_{j,n}=(N_{j,n}+N_{j,n-1})/2$.

(2) Mean viscosity[36]: Viscosity of component-j is calculated using Licht *et al.* equation by the use of critical temperature and pressure, $T_{c,j}$ and $P_{c,j}$, by

$$\bar{\mu}_{j,n}=2.268\times 10^{-3}\left(\frac{M_j^3 P_{c,j}^4}{T_{c,j}}\right)^{1/6}\left[\frac{(\overline{T}_n/T_{c,j})^{3/2}}{(\overline{T}_n/T_{c,j})+0.8}\right] \quad \text{kg/m·hr}$$

Mean viscosity of gases is calculated using Wilke equation.

$$\bar{\mu}_n=\sum_j \bar{\mu}_{j,n}/[1+(1/\bar{y}_{j,n})(\sum_{i\neq j}\bar{y}_{i,n}\phi_{j,i})]$$

where, $$\phi_{j,i}=[1+(\bar{\mu}_{j,n}/\bar{\mu}_{i,n})(M_i/M_j)^{1/4}]^2/(4/\sqrt{2})[1+(M_j/M_i)]^{1/2}$$

(3) Mean molar heat capacity at constant pressure:

$$\overline{C}_{p,n}=\bar{a}+\bar{b}\overline{T}_n+\bar{c}\overline{T}_n^2 \quad \text{kcal/kg-mol·°K}$$

where, $\bar{\alpha}=\sum_j \alpha_j \bar{y}_{j,n}(\alpha=a, b,$ and $c)$. The values of constants of heat capacity expressions for gaseous components, a_j, b_j, and c_j, are adopted from Nagasako *et al.*[32]

(4) Mean enthalpy of reaction:

$$(\overline{\Delta H})_n=(\overline{\Delta H_{298.16}})_n+(\overline{\Delta C_p})_n(\overline{T}_n-298.16)$$

where,
$$(\overline{\Delta H_{298.16}})_n=\sum_j(\Delta H_{f,298.16})_j(\Delta y_{j,n})$$
$$(\overline{\Delta C_p})_n=(1/6)[(\Delta C_{p,298.16})_n+4(\Delta C_{p,(\bar{T}_n+298.16)/2})_n+(\Delta C_{p,\bar{T}_n})$$
$$(\Delta C_{p,T})_n=\Delta a+(\Delta b)\,T+(\Delta c)\,T^2, \quad \Delta\alpha=\sum_j \alpha_j(\Delta y_{j,n}) \quad (\alpha=a, b, \text{and } c)$$
$$\Delta y_{j,n}=\Delta N_{j,n}/\sum_j \overline{N}_{j,n}, \quad \Delta N_{j,n}=N_{j,n}-N_{j,n-1}.$$

The values of $(\Delta H_{f,298.16})_j$ is adappted from Nagasako *et al.*[32].

(5) Mean heat conductivity of gas and wall: The mean heat conductivity of gaseous mixture is calculated using Eucken's equation[36].

$$(\bar{k}_g)_n=\bar{\mu}_n[(\overline{C}_p)_n+2.48]/\overline{M}_n \quad \text{kcal/hr·m·°C}$$

For mean heat conductivity of wall, the value of 18-8 stainless steel is applied[12].

$$(\bar{k}_w)_n = 9.65 + 0.0108\ \overline{T}_n \quad \text{kcal/hr·m·°C}$$

4.4 Results of calculations and discussion

4.4.1 Determination of number of reactor tubes The numbers of reactor tubes and exit conditions for various values of heat supply are shown in Table 16. For $q=27000$ kcal/hr·m², results obtained for various inlet gas pressures are also shown in Table 16. The results are compared in Fig. 9-1. The time of calculation was 20 seconds for each run by HITAC 5020 digital computer in Tokyo University. Fig. 9-1 is comparable with that reported by Perkins *et al.*[34] In our calculations, the tube number, n_E, did not vary with P_0 when it decreased from 5 to 4 atm. Increase in q from 27000 to 32000 kcal/hr·m², decreases n_E from 34 to 29. But, $(T_W)_E$ approached the limitting values of gas temperature.

TABLE 16. Number of Tubes and Exit Conditions for Constant Heat Supply

q [kcal/hr·m²]	P_0 [atm]	n_E [−]	τ_E [hr]	T_E [°K]	P_E [atm]	$X_{A,E}$ [−]	$(\overline{T_W})_E$ [°K]
27000	5.0	34	0.00196	1031	2.81	0.684	1051
	4.9	34	0.00161	1033	2.63	1.681	1052
	4.8	34	0.00186	1035	2.43	0.679	1054
	4.7	34	0.00181	1037	2.23	0.675	1056
	4.6	34	0.00176	1039	2.02	0.669	1058
	4.5	34	0.00171	1042	1.77	0.665	1061
22000	4.9	41	0.00226	1031	1.91	0.656	1046
32000	4.3	29	0.00140	1048	1.95	0.673	1070

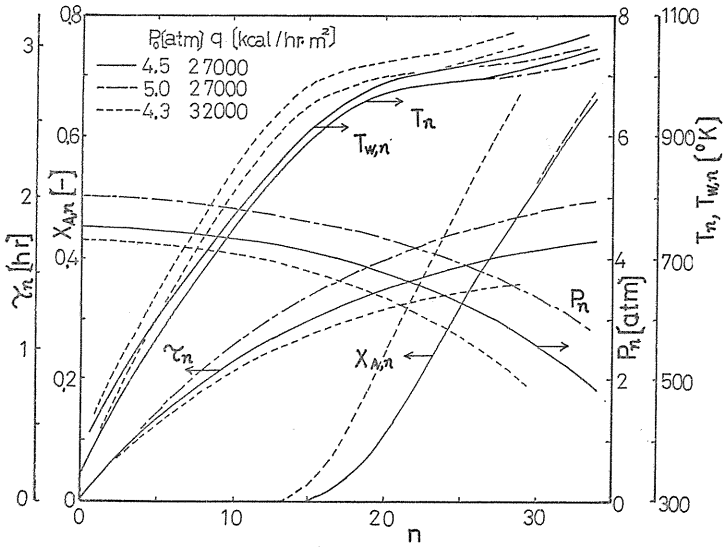

FIG. 9-1. Calculated curves for propane pyrolysis unit with constant heat flux.

The present results could not be compared with those of Snow *et al.*[43] and Andrews *et al.*[2], because their methods to obtaine initial conditions were not explained. However, our present method made the design accurate and simple by taking into consideration of the changes of moles of each component in each tube by calculating numerically the rate equations until the reactor volume reached to the volume of one tube and, thus, the expansion factor and the rate of reaction were obtained accurately with change in composition. The number of trial and error calculations was also decreased by assuming the initial values of mean temperature and pressur by the use of the changes in preceding tube.

4.4.2 Heat supply to wall Snow *et al.*[43] and Andrews *et al.*[2], respectively, changed the heat supply to each tube stepwise and continuously. For investigation of the effect of the heat supply scheme, we calculated for the cases where the

TABLE 17. Number of Tubes and Exit Conditions with Change in Heat Supply

Method A: $q_n = q_0 - (\Delta q)_n$ [kcal/hr·m²]

q_0	Δq	P_0	n_E	τ_E	T_E	P_E	$X_{A,E}$	$(\overline{T_W})_E$
32000	300	4.6	34	0.00168	1033	1.86	0.665	1048
22000	−300	4.5	34	0.00180	1047	1.95	0.670	1070

Method B: $q_n = q_0 (n \leqq 17)$, $q_n = q_0 - \Delta q (n > 17)$

q_0	Δq	P_0	n_E	τ_E	T_E	P_E	$X_{A,E}$	$(\overline{T_W})_E$
32000	10000	4.6	34	0.00163	1036	1.73	0.676	1036
22000	−10000	4.4	34	0.00180	1047	1.83	0.655	1070

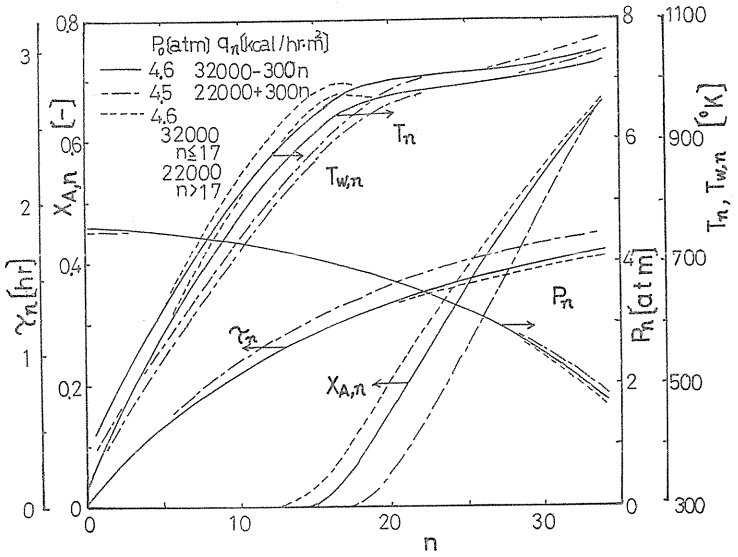

FIG. 9-2. Calculated curves for propane pyrolysis uuit with varying heat flux.

heat supply was changed in linearly and stepwise with tube number (call scheme A and B, respectively), keeping the mean of total heat supply at the constant 27000 kcal/hr·m^2 as adopted above. The results are shown in Table 17 and Fig. 9-2.

Tables 16 and 17 show that the total number of tubes, n_E, is kept constant irrespective of the heat flux distributions so far the mean of total heat supply is identical. However, Figs. 9-1 and 9-2 show that when the heat supply is decreased with increase in tube number, the slop of curve of conversion vs. tube number decreases. Thus, we can obtaine a stabilization condition at the exit for the concentrations of propylene and ethylene and the control of reactor becomes easier. These schemes have further benefits that the coke deposition and wall temperature rise in tubes near to the reactor exit are depressed. The difference in effects of schemes A and B is not remarkable. But, as the curves of wall temperature for scheme B have maximum points, scheme A may be superior.

5. Catalytic Cracking of Butane[18]

5.1 Derivation of stoichiometric equations and rate equations of butane cracking

5.1.1 Elementary carbonyl ion reactions of butane cracking Characteristic differences of catalytic cracking from thermal cracking are that the former is a milder reaction over acidic catalyst such as silica-alumina and proceeds through

TABLE 18. Elementary Carbonyl Ion Reactions and Rate Equations of Catalytic Cracking of Butane

Elementary Carbonyl reaction	Rate equation	
initiation step		
$C_4H_{10}+L\rightarrow C_4H_9^+\cdots LH^-$	$r_1=k_1C_An_L$	(1)
$C_4H_8+BH\rightarrow C_4H_9^+\cdots B^-$	$r_2=k_2C_Dn_{BH}$	(2)
$C_3H_6+BH\rightarrow C_3H_7^+\cdots B^-$	$r_3=k_3C_Pn_{BH}$	(3)
$C_2H_4+BH\rightarrow C_2H_5^+\cdots B^-$	$r_4=k_4C_Qn_{BH}$	(4)
propagation step		
$C_4H_9^+\rightarrow C_2H_4+C_2H_5^+$	$r_5=k_5C_A+$	(5)
$C_4H_9^+\rightarrow C_3H_6+CH_3^+$	$r_6=k_6C_A+$	(6)
$C_4H_9^+\rightarrow C_4H_8+H^+$	$r_7=k_7C_A+$	(7)
$C_3H_7^++C_4H_{10}\rightarrow C_3H_8+C_4H_9^+$	$r_8=k_8C_AC_F+$	(8)
$C_2H_5^++C_4H_{10}\rightarrow C_2H_6+C_4H_9^+$	$r_9=k_9C_AC_E+$	(9)
$CH_3^++C_4H_{10}\rightarrow CH_4+C_4H_9^+$	$r_{10}=k_{10}C_AC_M+$	(10)
$H^++C_4H_{10}\rightarrow H_2+C_4H_9^+$	$r_{11}=k_{11}C_AC_H+$	(11)
$2\,C_4H_8\rightarrow$coke $1+C_4H_{10}$	$r_{12}=k_{12}C_D^2$	(12)
$2\,C_3H_6\rightarrow$coke $2+C_3H_8$	$r_{13}=k_{13}C_P^2$	(13)
$2\,C_2H_4\rightarrow$coke $3+C_2H_6$	$r_{14}=k_{14}C_Q^2$	(14)
n-$C_4H_9^+\rightleftarrows$i-$C_4H_9^+$	$r_{15}=k_{15}C_{n\text{-}A}+-k_{15'}C_{i\text{-}A}+$	(15)
termination step		
i-$C_4H_9^+\cdots LH^-\rightarrow$i-$C_4H_{10}+L$	$r_{16}=k_{16}C_A+{}_{-LH}$	(16)
i-$C_4H_9^+\cdots B^-\rightarrow$i-$C_4H_8+BH$	$r_{17}=k_{17}C_A+{}_{-B}$	(17)

carbonyl ions as intermediates formed on the acidic centers of the catalyst. However, detailed invastigation of the elementary carbonyl ion reactions is lacking even for butane, which is the lightest hydrocarbon investigated for catalytic cracking.

The carbonyl ion mechanism of butane cracking is postulated as in Table 18, referring to the publications of elementary carbonyl ion reactions by Greensfelder *et al.*[9)10)] on various hydrocarbons, and of discussions for the cracking of *n*-dodecane and *n*-hexadecane by Kunugi *et al.*[20)], and of summaries by Hara[38)] and Ozaki[40)]. Carbonyl ions are formed from paraffins on Lewis acid centers and from olefines on Brönsted acid centers. The latter is formed easier than the former[40)]. Therefore, the elementary reactions (2)～(4), which are participated by cracking products, are added to the initiation reaction.

Isomarization reactions of carbonyl ions such as reaction (15) in Table 18 occur for propyl and butyl ions, and their stability increases in order of tertiary, secondary, and primary ions[38)40)]. But, as the isomerization reactions are faster than other elementary reactions[20)], we assumed equilibriums between carbonyl ion isomers. These isomerization reactions are inclusively represented by the elementary reaction (15). Therefore, the ratios of carbonyl ion isomer concentrations are implicitly included in rate parameters of stoichiometric rate equation introduced in next section.

Ion transfer reactions can arise for components other than butane. However, under the existence of a great quantity of butane, butyl ion may be produced in greater quantity than other ions. Therefor, we assumed the elementary reactions (8)～(11) as net reactions in presence of butane. The ion transfer reactions are eliminated in the derivation of the stoichiometric rate equations shown latter. Reactions (5)～(7) are adopted for the ion decomposition reactions, because other ions than butyl exist in small quantities. For termination, reactions (16) and (17) are postulated as representative reactions, because the iso-butyl ion exist in large quantity.

Coke formation is caused by autosaturations of olefines, which are in turn the hydrogen transfer reactions between molecules[40)]. Compositions of coke on acid centers is complex and vary with process time. Therefore, reactions (12)～(14) are adopted as representative reactions.

TABLE 19. Rate Equations from Elementary Carbonyl Ion Reactions

$\Re_A = -(r_1+r_8+r_9+r_{10}+r_{11}+r_{12})$	(1)
$\Re_{i-A} = r_{15}$	(2)
$\Re_D = -r_2+r_7-2r_{12}+r_{17}$	(3)
$\Re_F = r_8+r_{13}$	(4)
$\Re_P = -r_3+r_6-2r_{13}$	(5)
$\Re_E = r_9+r_{14}$	(6)
$\Re_Q = -r_4+r_5-2r_{14}$	(7)
$\Re_M = r_{10}$	(8)
$\Re_H = r_{11}$	(9)
$\Re_{C1} = r_{12}$	(10)
$\Re_{C2} = r_{13}$	(11)
$\Re_{C3} = r_{14}$	(12)
$\Re_L = -r_1+r_{16}$	(13)
$\Re_{BH} = -r_2-r_3-r_4+r_{17}$	(14)

5.1.2 Stoichiometric equations and rate equations From Table 18, rates for each component are derived as shown in Table 19. Applying the steady state assumption of carbonyl ions in Table 18, we can eliminate the rate of elementary reactions of ion transfer and termination, *i.e.*, r_8, r_9, r_{10}, r_{11}, r_{16}, and r_{17}, from equations in Table 19, using the same reasonings applied for propane pyrolysis

in Chapter 1. Then, the rate equations in Table 19 are transformed to those in Table 20. The rate equations in Table 20, in turn, are corresponded to the stoichiometric equations of the first column in Table 21 in the meaning as applied in Chapter 1. The rates of reactions for the stoichiometric equations are denoted as the second column and are expressed as the third column in Table 21.

TABLE 20. Rate Equations Applied Steady State Assumption of Carbonyl Ions

$\Re_A = -(r_1+r_3+r_4+r_5+r_6+r_7-r_{12})$	(1)
$\Re_{i-A} = r_1$	(2)
$\Re_D = r_3+r_4+r_7-2r_{12}$	(3)
$\Re_F = r_3+r_{13}$	(4)
$\Re_P = -r_3+r_6-2r_{13}$	(5)
$\Re_E = r_4+r_5+r_{14}$	(6)
$\Re_Q = -r_4+r_5-2r_{14}$	(7)
$\Re_M = r_6$	(8)
$\Re_H = r_7$	(9)
$\Re_{C1} = r_{12}$	(10)
$\Re_{C2} = r_{13}$	(11)
$\Re_{C3} = r_{14}$	(12)
$\Re_L = \Re_{BH} = 0$	(13)

Now, as the rate expressions of the third column in Table 21 yet include concentrations of carbonyl ions and of acid centers, some simplifying approximations are introduced. As the first approximation, the concentrations of carbonyl ions are expressed as propotional to the n-th power of the concentrations of each parent hydrocarbon as assumed for propane pyrolysis, *i.e.*, $C_{A+} \propto C_A^n$. The concentration of free Lewis acid centers, n_L, which are active for paraffins, increases with decrease in butane concentration, while the concentration of Brönsted acid centers, n_{BH}, which are active for olefines, decreases with increase in olefine concentrations. However, as our present experiments are made for high temperatures and the adsorption of molecules is less important. Therefore, we make the second approximation that n_L and n_{BH} are both proportional to C_A. Thus, the rate equations reduced to those of the last column in Table 21. From Table 21, the rates of production of each molecular species can be expressed as shown in Table 22.

TABLE 21. Stoichiometric Equations and Rate Equations of Catalytic Cracking of Butane

Stoichiometric equation	Rate equation			
initiation and termination step				
n-$C_4H_{10} \rightarrow$ i-C_4H_{10}	r_a	$k_1C_An_L$	$k_aC_A^n$	(1)
$C_4H_{10}+C_3H_6 \rightarrow C_4H_8+C_3H_8$	r_b	$k_3C_Pn_{BH}$	$k_bC_PC_A^{n-1}$	(3)
$C_4H_{10}+C_2H_4 \rightarrow C_4H_8+C_2H_6$	r_c	$k_4C_Qn_{BH}$	$k_cC_QC_A^{n-1}$	(4)
propagation step				
$C_4H_{10} \rightarrow C_2H_4+C_2H_6$	r_d	k_5C_A+	$k_dC_A^n$	(5)
$C_4H_{10} \rightarrow C_3H_6+CH_4$	r_e	k_6C_A+	$k_eC_A^n$	(6)
$C_4H_{10} \rightarrow C_4H_8+H_2$	r_f	k_7C_A+	$k_fC_A^n$	(7)
2 $C_4H_8 \rightarrow$ coke 1+C_4H_{10}	r_g	$k_{12}C_D^2$	$k_gC_D^n$	(12)
2 $C_3H_6 \rightarrow$ coke 2+C_3H_8	r_h	$k_{13}C_P^2$	$k_hC_P^n$	(13)
2 $C_2H_4 \rightarrow$ coke 3+C_2H_6	r_i	$k_{14}C_Q^2$	$k_iC_Q^n$	(14)

TABLE 22. Rate Equation of Catalytic Cracking of Butane in Terms of N_j

$$-dN_A/d\theta=\{(k_a+k_e+k_f)-k_g(N_D/N_A)^n+k_bN_P/N_A+k_cN_Q/N_A\}N_A^nV^{1-n} \quad (1)$$

$$dN_{i-a}/d\theta=k_aN_A^nV^{1-n} \quad (2)$$

$$dN_D/d\theta=\{k_f-2k_g(N_D/N_A)^n+k_bN_P/N_A+k_cN_Q/N_A\}N_A^nV^{1-n} \quad (3)$$

$$dN_F/d\theta=\{k_bN_P/N_A+k_h(N_P/N_A)^n\}N_A^nV^{1-n} \quad (4)$$

$$dN_P/d\theta=\{k_e-k_bN_P/N_A-2k_h(N_P/N_A)^n\}N_A^nV^{1-n} \quad (5)$$

$$dN_E/d\theta=\{k_a+k_cN_Q/N_A+k_i(N_Q/N_A)N_A^nV^{1-n} \quad (6)$$

$$dN_Q/d\theta=\{k_a-k_cN_Q/N_A-2k_i(N_Q/N_A)^n\}N_A^nV^{1-n} \quad (7)$$

$$dN_M/d\theta=k_eN_A^nV^{1-n} \quad (8)$$

$$dN_H/d\theta=k_fN_A^nV^{1-n} \quad (9)$$

5. 2 Experimentals

5. 2. 1 Experimental method Fig. 10 illustrates the apparatus used for the experiments of catalytic cracking of butane. The reactor for low temperature experiments is a 14 times coiled spiral Terex glass tube of 0.50 cm I.D. and 170 cm length, and that for high temperature experiments is a 9 times coiled quartz tube of 0.60 cm I.D. and 140 cm length. The reactor is placed in a fluidized sand bath of 6 cm I.D. and 40 cm height. The temperature is measured by a 0.3 mm chromel vs. alumel thermocouple at the outside surface of the reactor. Temperature difference between one-third and two-third position along the spiral reactor was less than 3°C and the mean temperature was adopted as the reactor temperature.

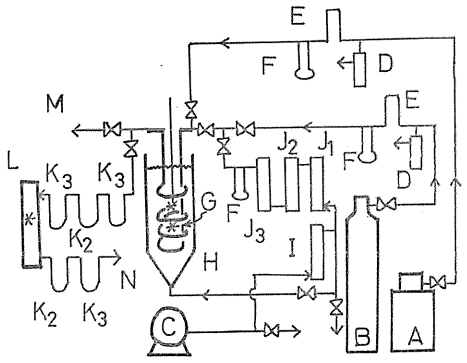

FIG. 10. Schematic diagram of catalytic cracking apparatus.
A: butane, B: nitrogen, C: blower, D: pressur controller, E: flow controller, F: olifice flow meter, G: reactor, H: fluidized sand bath, I: deoiler, J_1: silica gel, J_2, K_2: soda lime, K_3, J_3: magnesium perchlorate, L: cupuric oxide, M, N: exhaust, ∗: thermocouples.

Butane of pure grade was obtained from Takachiho and Co.

Powdered 13%-alumina-silica catalyst from Shokubai Kasei and Co. is compressed to 5×5 mm cylindrical pellets with tablet machine. After breaking and sieving, a fraction of 0.50~0.86 mm granules is collected and used as catalyst. Weights of catalyst applied for low and high temperature experiments were 14.34 and 13.95 g, respectively. The catalyst was regenerated for 1~5 hrs in flowing air at 550~600°C. Good reproducibilities were obtained.

Gaseous products from the reactor were analyzed by gas chromatography. Column of activated alumina with 1.0% squalane 4.5 m length was used at 70°C. Hydrogen was used as carrier gas for measurement of methane, ethane, ethylene, propane, propylene, butane, and butylene, and nitrogen was used for measurement of hydrogen. Both measurements were correlated by taking the methane quantity

as a standard.

Liquid products of yellow brown colur were observed on the wall at the exit of the reactor. But, the quantities were so small as we could not detect their composition.

5. 2. 2 Investigations of coke Quantities and compositions of coke were measured by combusting of the coke at 600°C in air flow of about 30 cc/min for 5~7 hrs. Total quantities of coke were determined from the weight differences of the reactor before and after the combustion. In order to determine the compositions, exhaust gases of combustion were passed through absorption tubes, as illustrated at the left hand side in Fig. 10. Water vapour was absorbed by the first magnesium perchlorate tube and then carbon dioxide by the first soda lime tube. After passing through the second magnesium perchlorate tube to ensure the absorption of water vapour, the exhaust gas was passed over cupric oxide at 400°C to convert carbon monoxide to dioxide. The gases were then passed through the second soda lime tube and finally the third magnesium perchlorate tube. Quantities of water and carbon dioxide produced by the combustion were determined from the weight increases of magnesium perchlorate and soda lime tubes, respectively.

The quantity of coke per unit weight of catalyst, W_C, and the atomic ratio of hydrogen to carbon, m/n, are shown, respectively, against the process time of cracking, t_p, in Figs. 11 and 12. The quantities of coke determined from the weight differences of reactor and the sum of weights of hydrogen and carbon determined from weights of water and carbon dioxide show good agreement each other, and increase with process time as seen from Fig. 11.

As seen from Fig. 12, the atomic ratio of hydrogen to carbon decreases at first with increase in process time, and becomes constant at 0.3~0.4 at 600°C for large process time. From the compositions of coke, the coke may be considered to be polycyclic aromatics whose composition varies with depositing condition.

The effect of coke deposition on conversion of butane was investigated by tracing the change of product composition with process time. Fig. 13 shows

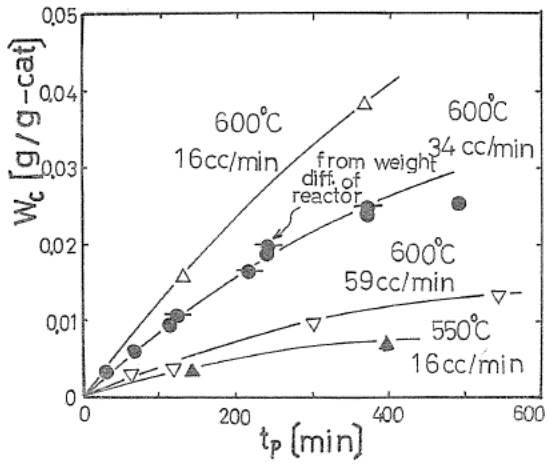

FIG. 11. Changes of coke deposit with process time.

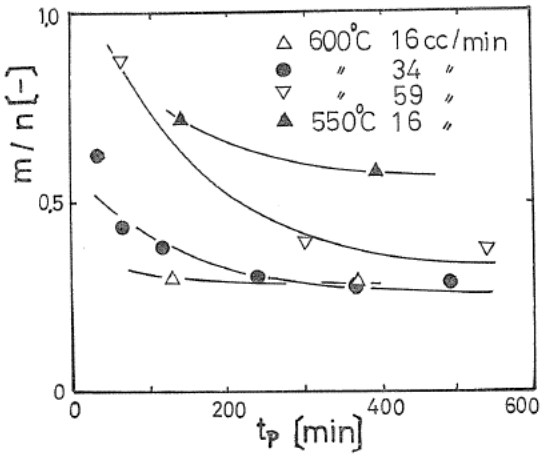

FIG. 12. Changes of ratio of hydrogen to carbon of coke with process time.

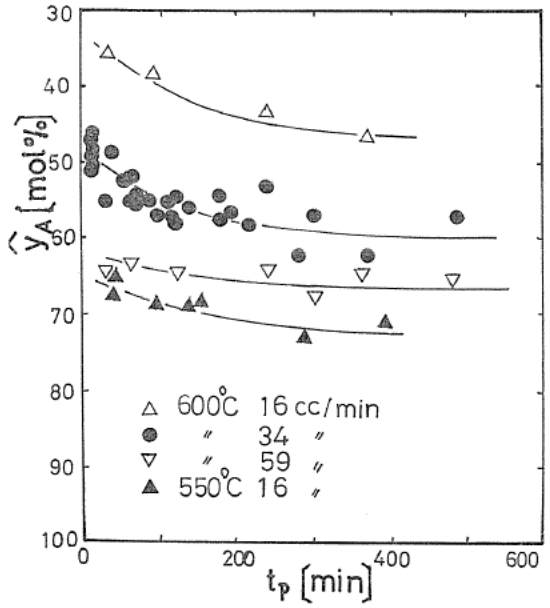

FIG. 13. Changes of mole percent of butane in measurable gases by gas chromatography with process time.

the relations between percentage of butane in product gases as measured by chromatography and the process time. At 600°C and feed rate of butane of 34 cc/min, the conversion of butane decreases rapidly for an initial period of process, but becomes almost at constant after 100 min.

The atomic ratio of hydrogen to carbon was investigated by several other authors. Kunugi *et al.*[20] suggested values less than 1 and Weisz *et al.*[47] gave values between 1.0 and 0.4. The later authors and Massoth *et al.*[25] found decrease

of the ratio at high temperature. Those findings are qualitatively coincide with our present researches.

5.2.3 Products distribution Mole percent distribution of products measured by the gas chromatography are shown against mole percent of butane in Figs. 14-1 and 14-2 for temperature between 600 and 610°C. The solid lines in Figs.

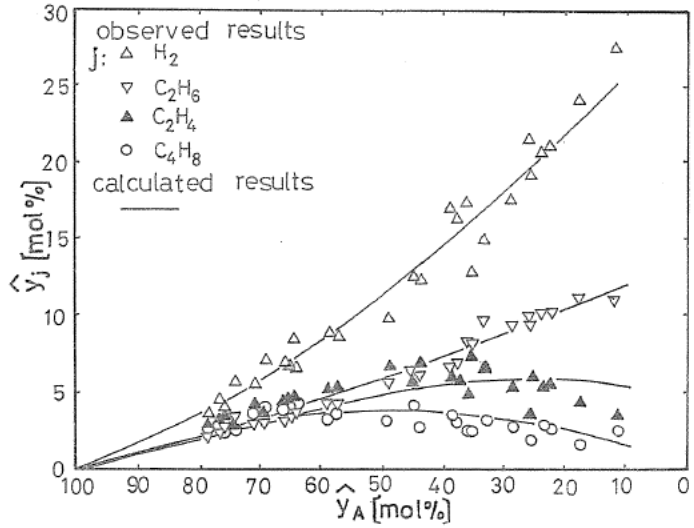

FIG. 14-1. Observed and calculated correlations of molar percentage of products vs. butane for catalytic cracking of butane (1).

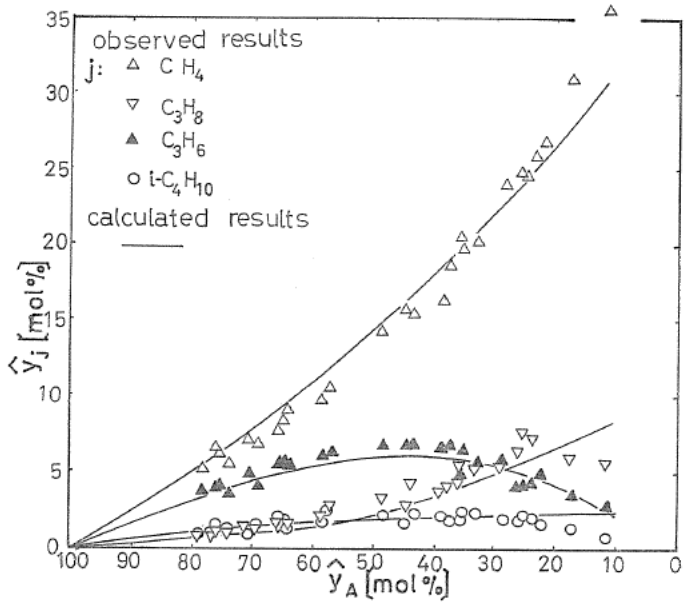

FIG. 14-2. Observed and calculated correlations of molar percentage of products vs. butane for catalytic cracking of butane (2).

14–1 and 14–2 are those calculated as described later. Table 23 shows the comparison of the product distributions of thermal and catalytic cracking of butane. Table 23 shows that for catalytic cracking the reactions to form propane and iso-butane are important.

In order to investigate the effect of secondary reactions, catalytic crackings of each one of hydrocarbons produced by butane cracking were studied. Table 24 shows the results. The olefines, such as butene, propylene, and ethylene, were cracked more easily than the corresponding parafin hydrocarbons. Distributions of main products were approximately $CH_4 : H_2 : C_4H_{10} = 2 : 2 : 1$ for butene, $CH_4 : H_2 : C_3H_8 = 1 : 1 : 1$ for propylene, and $CH_4 : H_2 : C_2H_6 = 1 : 1 : 2$ for ethylene.

TABLE 23. Product Distributions of Thermal and Catalytic Cracking of Butane

W	t	v_0	$\hat{y}_j$ [mol%]								
[g-cat]	[°C]	[cc/min]	CH_4	C_2H_6	C_2H_4	C_3H_8	C_3H_6	i-C_4H_{10}	C_4H_{10}	C_4H_8	H_2
14.34	600	33.3	10.4	4.0	5.4	2.7	6.4	2.1	57.0	3.6	8.4
14.34	607	9.6	26.0	10.2	5.3	7.1	4.4	1.9	23.5	1.7	20.1
—	616	32.4	12.1	4.4	8.0	0.1	11.9	0.0	60.1	1.0	2.3
—	641	22.8	25.1	7.3	17.2	0.4	18.9	0.0	23.8	1.3	6.1

TABLE 24. Product Distributions of Catalytic Cracking of Hydrocarbons Produced by Butane Cracking, $W = 13.95$ g-cat

Feed HC	t	v_0	$\hat{y}_j$ [mol%]								
	[°C]	[cc/min]	CH_4	C_2H_6	C_2H_4	C_3H_8	C_3H_6	i-C_4H_{10}	C_4H_{10}	C_4H_8	H_2
C_2H_6	603	50.4	0.4	96.1	6.9	0.9	—	—	—	—	1.7
C_3H_8	600	47.4	4.0	1.1	3.5	78.7	3.1	0.2	5.0	—	4.3
i-C_4H_{10}	601	40.2	12.7	1.3	2.4	3.1	8.6	46.5	2.5	7.2	15.7
C_2H_4	603	43.2	10.7	17.6	50.6	2.6	5.8	1.1	1.9	—	9.8
C_3H_6	603	43.2	23.2	5.1	4.5	20.5	23.2	0.9	1.1	—	21.5
l-C_4H_8	602	42.6	28.0	6.8	3.1	4.0	9.5	1.6	7.2	16.3	23.6
i-C_4H_8	603	48.6	23.6	2.3	1.3	2.4	6.0	12.4	2.1	27.0	22.9

5.2.4 Rate of butane disappearance For the evaluation of conversion of butane from the product distributions of exit gases, we need to assume coke compositions. Then, the expansion factor for each run can be calculated using mass balances of carbon and hydrogen atoms. Here, the coke includes all components which are not measured by gas chromatography, *i.e.*, not only the coke deposited at the active centers of catalyst as mesured in last section, but also the yellow brown liquid products at the wall of exit of reactor and volatile liquid and gaseous products which can not be analyzed by the gas chromatography. Although, the ratio hydrogen to carbon of coke deposited on the active centers is less than 1 at 600°C, this coke is a small part of the total coke. Therefore, we assumed the mean composition of the total coke as C_4H_6 for experimental conditions applied here.

When first- and second-order rate equations are assumed for butane disap-

pearance, the integral rates are expressed by Eqs. (26) and (27), respectively.

$$(1+\varepsilon_A)\ln[1/(1-X_A)]-\varepsilon_A X_A = k_{t,1}C_{A0}(W/F_{A0}) \quad (26)$$

$$2\varepsilon_A(1+\varepsilon_A)\ln(1-X_A)+\varepsilon_A^2 X_A+(\varepsilon_A+1)^2 X_A/(1-X_A) = k_{t,2}C_{A0}^2(W/F_{A0}) \quad (27)$$

where, $k_{t,1}$ and $k_{t,2}$ are the first- and second-order rate constants based on unit weight of catalyst. The expansion factor, ε_A, was not constant and increased with increase in conversion of butane.

Fig. 15 illustrate the Arrhenius plots of $k_{t,1}$ and $k_{t,2}$. From Fig. 15, we obtaine

$$k_{t,1} = 1.57\times10^5 \exp(-28300/RT) \quad \text{cc}\cdot\text{g-cat}^{-1}\cdot\text{sec}^{-1} \quad (28)$$

$$k_{t,2} = 2.41\times10^{12} \exp(-36800/RT) \quad \text{cc}^2\cdot\text{g-cat}^{-1}\cdot\text{mol}^{-1}\cdot\text{sec}^{-1} \quad (29)$$

Franklin *et al.*[20] obtained 26.3 kcal/mol for activation energy, assuming three-half-order at 450~500°C. In Fig. 15 second-order rate constants scatter at high temperature. Therefore, we apply the first-order kinetics in the following calculations.

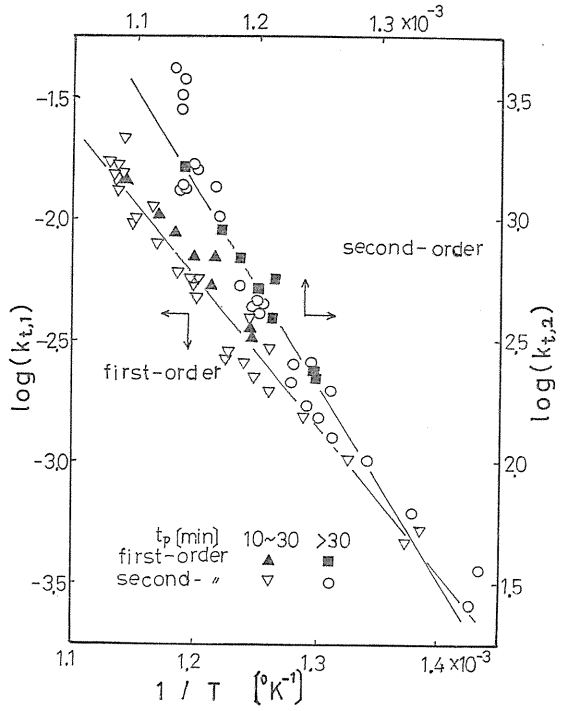

FIG. 15. Arrhenius plots of first- and second-order rate constants for catalytic cracking of butane.

5.3 Calculation of optimum rate parameters

The rate parameters of the stoichiometric equations in Table 22 were calculated, assuming $n=1$, from the experimental results of product distributions for the butane cracking in Figs. 14-1 and 14-2. Experimental values applied for the

calculations were $J=9$ ($j=$A, $i-$A, D, F, P, E, Q, M, and H), $P=9$, and $I=27$. For the catalytic cracking of butane, the relation between the moles of j-th compornents based on 100 moles of feed butane, N_j, and the conversion of butane, X_A, can not be determied uniquely as for propane pyrolysis, because the higher quantity of coke inhibites the analysis. Therefore, we applied relative values of the moles of j-th components $\hat{y}_j$, *i.e.*, molar concentrations of components as measured by gas chromatography and shown in Figs. 14-1 and 14-2, to the rate equations in Table 22 to detemine optimum values of parameters.

The optimum values were calculated by the Marquardt method decreasing the weighting factor with every iteration, *i.e.*, method E'.

The values obtained are shown in the third column of Table 25. Initial values of parameters were taken as 1 for k_d, k_c, and k_f which respected on butyl ion decomposition reaction and for other parameters were taken as 1/100. The time step for numerical integration of rate equations was $\Delta\theta=0.001$. The rerative values of parameters were converted to $k_e=1.00$ as standard for each iteration. The time of calculations was 8 min with FACOM 230-60 digital computer in Kyoto University.

As shown in Table 25, the resulted values were negative for k_b and k_c. This may be caused by that, in stoichiometric equations in Table 21, we assumed Eqs. (13) and (14) for coke formation by which large quantities of propane and ethane were formed. Table 24 shows that the propylene and butene cracking, respectively, produce large quantities of methane and hydrogen. Therefore, we modify the coke formation reactions as in Table 26. Then, the stoichiometric rate equations in Table 22 are modified to the rate equations in Table 27. The values of rate parameters evaluated for the rate equations in Table 27 are show in the last

TABLE 25. Rate Parameters of Catalytic Cracking of Butane, After Six Iterations. $k_e=1.000$ (Standard)

k_p	Initial	Table 22	Initial	Table 27
k_a	0.1	0.009	0.1	0.137
k_b	0.1	−2.898	0.1	3.656
k_c	0.1	−1.661	0.1	1.437
k_d	1.0	0.401	1.0	0.485
k_f	1.0	0.796	1.0	0.696
k_g	0.1	1.659	0.1	1.664
k_h or k_{ha}	0.1	5.020	0.1	6.688
k_i or k_{ia}	0.1	1.632	0.1	1.734
σ_{Nj}	6.379	1.202	6.244	1.228

TABLE 26. Replacements of Reactions (13) and (14) of Coke Formation in Table 21

Stoichiometric equation	Rate equation	
$2\,C_4H_8 \rightarrow$ coke $2+CH_4+H_2$	$r_{ha}\quad k_{ha}C_D^n$	(13 *a*)
$2\,C_3H_6 \rightarrow$ coke $3+CH_4+H_2$	$r_{ia}\quad k_{ia}C_P^n$	(14 *a*)

TABLE 27. Modified Rate Equations

$$-dN_A/d\theta=\{(k_d+k_e+k_f)-k_g(N_D//N_A)^n+k_bN_P/N_A+k_cN_Q/N_A\}N_A^nV^{1-n} \quad (1)$$

$$dN_{i-A}/d\theta=k_aN_A^nV^{1-n} \quad (2)$$

$$dN_D/d\theta=\{k_f-2(k_g+k_{ha})(N_D/N_A)^n+k_bN_P/N_L+k_cN_Q/N_A\}N_A^nV^{1-n} \quad (3)$$

$$dN_F/d\theta=\{k_bN_P/N_A\}N_A^nV^{1-n} \quad (4)$$

$$dN_P/d\theta=\{k_e-k_bN_P/N_A-2k_{ia}(N_P/N_A)^n\}N_A^nV^{1-n} \quad (5)$$

$$dN_E/d\theta=\{k_d+k_cN_Q/N_A\}N_A^nV^{1-n} \quad (6)$$

$$dN_Q/d\theta=\{k_d-k_cN_Q/N_A\}N_A^nV^{1-n} \quad (7)$$

$$dN_M/d\theta=\{k_e+k_{ha}(N_D/N_A)^n+k_{ia}(N_P/N_A)^n\}N_A^nV^{1-n} \quad (8)$$

$$dN_H/d\theta=\{k_f+k_{ha}(N_D/N_A)^n+k_{ia}(N_P/N_A)^n\}N_A^nV^{1-n} \quad (9)$$

column of Table 25. Negative values of rate parameters are disappeared. The plots of $\hat{y}_j$ vs. $\hat{y}_A$ are shown by the solid lines in Figs. 14-1 and 14-2.

Conclusions

1. For the complex reaction of thermal cracking of propane composed of multiple elementary reaction steps including free radicals as intermediates, a method was introduced to derive a set of convenient stoichiometric equations and conjugate rate equations which include terms of chemically measurable species only. Modification method was also considered to express the retardation effect of propylene.

2. Experimental reseaches of the propane pyrolysis were conducted. Expansion factor of the reaction and absolute mole numbers of product species were calculated from relative concentrations of products obtained by gas chromatography and the mass balances of hydrogen and carbon atom. Rate equation of propane disapperance was also introduced. Effects of addition of propylene in feed propane was examined.

3. Gauss, steepest descent, and Marquardt method were comparatively examined in their efficiencies to determine optimum values of parameters of complex simultaneous rate equations of propane pyrolysis. When good initial values of parameters have been obtained by some means such as analog simulation, Gauss method applied for integral reaction rates gives the smallest value of standard deviation. But, otherwise, Marquardt method applied with decreasing weighting factor for every iteration gives the best results.

4. Applicability of the stoichiometric rate equations to pyrolysis furnace design was illustrated by sample calculations. An improved method for designing a multiple tubular reactor was presented, where the mean temperature and pressure in each tube were assumed by extrapolations of those of preceding tube for evaluations of physical constants, and the expansion factor and changes in mole numbers of each component were calculated by numerical integration of the rate equations.

5. Derivation of stoichiometric rate equations was applied for catalytic cracking of butane. Optimum values of parameters were evaluated by the use of integral rates experimentally determined. Coke deposition and its composition were determined experimentally, and its effect on the rate of reaction were discussed.

Literature cited

1) Amano, A. and M. Uchiyama: *J. Phys. Chem.*, 1963, **67**, 1242.
2) Andrews, A. J. and L. W. Pollock: *Ind. Eng. Chem.*, 1959, **51**, 129.
3) Bach, G. and S. Nowak: *Chem. Techn.*, 1967, **19**, 161.
4) Ball, W. E. and L. C. D. Greenweghe: *Ind. Eng. Chem., Fundamentals*, 1966, **5**, 181.
5) Benson, A. M.: *A. I. Ch. E. Journal*, 1967, **13**, 903.
6) Buekens, A. G. and G. F. Froment: *Ind. Eng. Chem., Process Design and Dvelop*, 1968, **7**, 435.
7) Fair, J. R. and H. F. Rase: *Chem. Eng. Progr.*, 1954, **50**, 415.
8) Franklin, J. L. and D. E. Nicholson: *J. Phys. Chem.*, 1956, **60**, 59.
9) Greensfelder, B. S. and H. H. Voge: *Ind. Eng. Chem.*, 1945, **37**, 514, 983, 1038.
10) Greensfelder, B. S., H. H. Voge, and G. M. Good: *ibid.*, 1945, **37**, 1168; 1949, **41**, 2573.
11) Hirado, M. and S. Yoshioka: Preprint 33th Annual Meeting, Soc. Chem. Eng. Japan., Bd. 1, p. 260, Kyoto, 1968.
12) Kagaku Kogaku Kyokai (Soc. Chem. Eng. Japan): Kagaku Kogaku Benran (Handbook of Chem. Eng.), Maruzen & Co., 1958.
13) Kershenbaum, L. S. and J. J. Martin: *A. I. Ch. E. Journal*, 1967, **13**, 148.
14) Kubota, K. and N. Morita: *Kogyo Kagaku Zasshi* (*J. Chem. Soc. Japan, Ind. Chem. Sec.*), 1969, **72**, 616.
15) Kubota, K. and N. Morita: *ibid.*, 1969, **72**, 2522.
16) Kubota, K. and N. Morita: *Kagaku Kogaku* (*Chem. Eng. Japan*), 1970, **34**, 612.
17) Kubota, K. and N. Morita: Preprint 3rd Autumn Meeting, Soc. Chem. Eng. Japan, p. 81, Osaka, 1969.
18) Kubota, K. and N. Morita: Proceedings 8th General Meeting, Soc. Chem. Eng. Japan, Section 2, p. 35, Nagoya, 1969.
19) Kunii, D. and S. Okayasu: *Kagaku Kogaku* (*Chem. Eng. Japan*), 1967, **31**, 800.
20) Kunugi, T., K. Fujimoto, and T. Sakai: *Sekiyu Gakkai Shi* (*J. Japan Petrol. Inst.*), 1968, **11**, 103, 696.
21) Kunugi, T., and T. Sakai, K. Soma, and Y. Sasaki: *Kogyo Kagaku Zasshi* (*J. Chem. Soc. Japan, Ind. Chem. Sec.*), 1968, **71**, 689.
22) Kunugi, T., K. Soma, and T. Sakai: *ibid.*, 1968, **71**, 839.
23) Laidler, K. J. and B. W. Wojiciechowski: *Proc. Roy. Soc.* (*London*), 1960, **A 259**, 257; 1961, **A 260**, 91.
24) Laidler, K. J., N. H. Sagert, and B. W. Wojciechowski: *ibid.*, 1962, **A 270**, 242.
25) Lichtenstein, I.: *Chem. Eng. Progr.*, 1964, **60** (12), 64.
26) Marek, L. F. and W. B. McCler: *Ind. Eng. Chem.*, 1931, **23**, 878.
27) Marqurdt, D. W.: *J. Sos. Ind. Appl. Math.*, 1963, **11**, 431.
28) Massoth, F. E. and Menon, P. G.: *Ind. Eng. Chem., Process Design and Develop.*, 1969, **8**, 383.
29) Mezaki, R. and J. B. Butt: *Ind. Eng. Chem., Fundamentals*, 1968, **7**, 120.
30) Morita, N.: *Kagaku Kogaku* (*Chem. Eng. Japan*), 1970, **34**, 464.
31) Morita, N. and K. Kubota: *Kemikaru Enjiniaringu* (*Chem. Eng.*), 1969, **14** (12), 49.
32) Nagasako, N., K. Sato, and R. Kiyoura: Kogyo Kagaku Keisanho, Hirokawa Book & Co., 1955.
33) Paul, R. E. and F. L. Marek: *Ind. Eng. Chem.*, 1934, **26**, 454.
34) Perkins, T. K. and H. F. Rase: *Chem. Eng. Progr.*, 1965, **52**, 105 M.
35) Purnell, J. H. and C. P. Quinn: *Proc. Roy. Soc.* (*London*), 1962, **A 270**, 267.
36) Sato, K.: Bussei Zyosu Suisanho, Maruzen & Co., 1954.
37) Schutt, H. C.: *Chem. Eng. Progr.*, 1947, **43**, 103.
38) Sekiyu Gakkai (Japan Petrol. Inst.): Bunkai, Sanka (Cracking and Oxidation), Asakura Book & Co., 1962.
39) Shirotsuka, T., A. Hirata, K. Kawasaki, and M. Chao: *Kagaku Kogaku* (*Chem. Eng. Iapan*), 1969, **33**, 662.

40) Shokubai Gakkai (Catalysis Soc. Japan): Shokubai Kogaku Koza (Handbook of Catal. Eng.), Vol. 7, Chizin Book & Co.. 1964.
41) Snow, R. H.: *J. Phys. Chem.*, 1966, **70**, 2780.
42) Snow, R. H., R. E. Peck, and C. G. Fredersdorff: *A. I. Ch. E. Journal*, 1959, **5**, 304.
43) Snow, R. H. and H. C. Schutt: *Chem. Eng. Progr.*, 1957, **53**, 133 M.
44) Tominaga, H., S. Abiko, and T. Kunugi: *Sekiyu Gakkai Shi* (*J. Japan Petrol. Inst.*), 1967, **10**, 190.
45) Tominaga, H., E. O'Shima, S. Abiko, T. Ohno, K. Uehara, and T. Kunugi: *Kagaku Kogaku* (*Chem. Eng. Japan*), 1969, **33**, 393.
46) Wang, Yui-Loong, R. G. Rinken, and W. H. Corcoran: *Ind. Eng. Chem., Fundamentals*, 1963, **2**, 161.
47) Weitz, P. B. and R. B. Goodwin: *J. Catal.*, 1966, **6**, 227.

Errata

Vol. 23, No. 1, page 89~91.

Change carbonyl to carbonium.